Title

Hydraulic Microhabitats at a Regulated River Confluence Influence Chinook Salmon Migratory Routing During Drought

Authors

Luis, Sean

Pasternack, Gregory B

Publication Date

2024

DOI

10.1002/eco.2727

Ecohydrology

WILEY

RESEARCH ARTICLE OPEN ACCESS

Hydraulic Microhabitats at a Regulated River Confluence Influence Chinook Salmon Migratory Routing During Drought

Sean Luis | Gregory B. Pasternack

Department of Land, Air, and Water Resources, University of California at Davis, Davis, California, United States

Correspondence: Sean Luis (smluis@ucdavis.edu; sean.luis@fishsciences.net)

Received: 30 December 2023 | **Revised:** 8 May 2024 | **Accepted:** 8 September 2024

Funding: This work was supported by Chapter 33 Post 9/11 G.I. Bill through the U.S. Department of Veterans Affairs; National Institute of Food and Agriculture; University of California, Davis; Western Division of the American Fisheries Society; Diablo Valley Fly Fishermen.

Keywords: anadromous fish | climate change | drought management | random forest model | river hydraulics

ABSTRACT

Successful upstream adult migration of Pacific salmon (*Oncorhynchus spp.*) from estuary to spawning grounds is critical to population recovery, especially during increasingly extreme droughts that degrade migratory habitat. In regulated systems, river confluences can pose significant navigation impediments given complex operational flow release criteria and other cumulative effects. Differing discharge magnitudes and ratios between tributaries may cause divergent confluence hydraulics and hydraulic microhabitat selectivity, influencing migratory routing. This study asks with respect to confluences: (1) Do magnitudes of discharge in each confluence tributary (and resulting combined discharge) influence availability of preferred hydraulic microhabitats in one river versus the other? (2) Does the ratio of discharge magnitudes influence availability of preferred hydraulic microhabitats in one river versus the other? We used data collected from California Central Valley fall-run Chinook salmon (*Oncorhynchus tshawytscha*) at the confluence of the Feather and Yuba Rivers as a model system to investigate. We combined observations of migratory behavioural responses to hydraulic microhabitats from dual-frequency identification sonars, spatially explicit, meter-resolution hydrodynamic modelling, and machine learning to generate a hydraulic microhabitat selectivity index and simulate upstream migratory pathways for nine pertinent discharge scenarios with four discharge ratios. Statistically significant ($p < 0.01$) differences in preferred hydraulic habitat were found among both discharge scenarios and ratios, with the Feather River selected in five out of nine scenarios. Discharge magnitude and ratio act as controls on distribution of preferred hydraulic microhabitats, and under certain conditions relevant to drought operations in this system, they can influence migratory routing and propensity of straying.

1 | Introduction

1.1 | Background

1.1.1 | Climate Change and Drought

Climate change poses significant threats to aquatic ecosystems due to extensively modified natural flow and thermal regimes to which organisms have adapted in recent millennia. In particular, increased duration and magnitude of drought conditions has changed the ecology of many landscapes across the world (Trenberth 2011). As noted by Cook, Mankin, and Anchukaitis (2018), drought signals manifest as a complex, interconnected web of environmental variation; linking climatic forcing to droughts can be a complicated task where landscape attributes of specific geographic regions must be accounted for (e.g., topography, snowpack, groundwater residence time and aquifer capacity, vegetation, biological communities, human

land uses and human demands on surface and subsurface water resources). Pacific salmon species occupy latitudes ranging from Central California (37° N) to coastal streams in northern Alaska and Russia (70° N), all of which are subject to some degree of drought-related impacts in the 21st century, according to widely accepted statistical projections (Caretta et al. 2022; Dai, Zhao, and Chen 2018; Xu et al. 2019). Climatic projections for California suggest that hydrologic droughts will be exacerbated through increased air temperatures from October–March and increased freezing elevations throughout winter periods leading to less snowpack and a continued shift toward rain-driven annual streamflow regimes throughout the state (Dai, Zhao, and Chen 2018; He et al. 2021; Ishida et al. 2018). Sun et al. (2019) estimate a 47–89% loss of overall snowpack in the Sierra Nevada in the month of March by the end of the 21st century.

Today, many Pacific salmon populations also inhabit catchments that have experienced varying degrees of fragmentation and hydrologic alteration due to water storage and conveyance infrastructure with the added complication that water resources are managed for a variety of human uses (Acreman et al. 2009; Magilligan and Nislow 2005). Management criteria for reservoir operations typically include provisions for drought events that attempt to sustain systems and processes that depend on certain minimum flows, including fish species that may also receive additional regulatory protection under the U.S. federal Endangered Species Act, Canadian Species At Risk Act, the Japanese River Act of 1964, or other state or local conservation laws (Di Baldassarre et al. 2017; Good et al. 2007; Irvine et al. 2005; Suzuki 2006). Minimum baseflows and drought operation criteria are often established for a regulated river on an individual-river basis based on its historical hydrograph and anticipated seasonal needs for water diversion.

1.1.2 | Emergence of Eflows and Ecohydraulic Methods

Development of species- and even life stage-specific environmental flow (i.e., eflow) criteria can be highly contentious. Many regulatory actions to secure allocations of stored water for such prescribed flows have been met with stakeholder resistance and legal action (Fisher, Michael Hanemann, and Keeler 1991; Horne et al. 2017; Lackey 2017; Tharme 2003). Despite such external pressures, in a growing number of countries, fishery managers must generate environmental flow schedules using the best available science to achieve habitat conditions most beneficial for the target species or life stage in question. Targets for habitat quality and function must then fit into a broader constellation of conservation goals such as enhancing population productivity or abundance metrics, conserving population structure, or addressing bottlenecks for mortality at vulnerable lifecycle stages.

Accessibility to two-dimensional (2D) hydrodynamic modelling software and recent advancements in the field of ecohydraulics (Pasternack 2019a, 2019b) have enhanced the potential for developing salmon habitat models that aid in drought planning and development of environmental flow criteria by making predictions about a variety of important individual ecological functions. For example, Benjankar et al. (2018) developed an integrated ecohydraulic modelling framework combining models of catchment hydrology, existing salmonid habitat models and an analysis of channel hydraulics to assess whether strategic dam operations might be able to mitigate climate change impacts to riverine fishes in the South Fork Boise River (Idaho, USA). Schwindt et al. (2019) developed River Architect, an ecohydraulics-based modelling framework that includes fish stranding risk analysis, cottonwood seedling recruitment potential prediction, microhabitat mapping and seasonal abundance quantification, lifespan prediction for several river restoration techniques and river project financial cost estimation. This framework did not include a migratory routing component.

1.1.3 | Importance of Confluences

Confluences are locations where a tributary channel meets a mainstem channel, forming a junction. They represent complex hydraulic and geomorphic features within fluvial channel networks. Significant improvements have been made in understanding the physical and biological implications of these features since the mid-20th century (Gualtieri et al. 2017; Miller 1958; Richards 1980). As key features of migratory habitat for riverine fishes, the physical processes at play ultimately drive habitat functionality in space and time. For example, discharge ratio, upstream bed slopes and channel junction angle are important drivers of bed morphology in the immediate up and downstream areas of confluences (Best 1986, 1988; Boyer, Roy, and Best 2006; Penna et al. 2018). Bed morphology at confluences then directly affects mixing processes with implications for fish migration cuing (Constantinescu et al. 2016; Gaudet and Roy 1995). A recent review by Yuan et al. (2022) highlights that confluences also represent longitudinal hotspots for ecological change in a river network with adjoining rivers potentially diverging in thermal regime, suspended sediment load, bed load, nutrient concentrations, water chemistry and organic matter content.

Major rivers are managed for competing interests under complex legal statutes that often have layered local, state and federal regulatory oversight (Bernazzani, Bradley, and Opperman 2012; Hillman 2009; Lorenz, Cofino, and Gilbert 2001; Moore, Maclin, and Kershner 2001; Zhang, Jin, and Yu 2018). As a result, a confluence of two major rivers may experience very different discharges from each river during low flow periods. A Chinook salmon (*Oncorhynchus tshawytscha*) escapement statistical analysis indicated that discharge magnitude and ratio between two major rivers can have a strong influence on migratory routing and can lead to instances of high straying rates (such as the 6:1 discharge magnitude ratio reported by YARMT 2013). In such cases, it is important to recognize that while discharge magnitude has been used to correlate reach- and catchment-scale patterns of adult salmon migration (Dahl et al. 2004; Hasler et al. 2014; Jager and Rose 2003), it cannot be used on its own to explain the abiotic–biotic mechanism linking complex migratory responses to confluence physicochemical conditions, because it is a system input, not a mechanism in and of itself; how that input drives the system (alone and combined with other drivers) requires detailed investigation.

1.1.4 | Prediction of Upstream Migration

The few habitat suitability curves for migrating adult salmon have varying survey methods, inconsistent results, and are

decades old (Table 1). Radio telemetry surveys were done on the Kenai River in Alaska for late summer-run Chinook salmon (Burger et al. 1983). Snorkel surveys for spring-run Chinook salmon were used in the Wind River, a tributary to the Columbia River in Washington State (Wampler 1986) and for fall-run Chinook salmon in the Stanislaus River, California (Aceituno 1990). These studies indicate that non-random hydraulic microhabitat selection occurs in migrating adult salmon. Thus, micro-scale hydraulic conditions at a confluence may partially influence migratory navigational choices. However, the added habitat complexity at a confluence along with differences in peak velocity and depth among existing HSCs for migrating adult Chinook salmon preclude their use in our study.

1.1.5 | Central Valley, California Context

Migratory habitat for Chinook salmon in California's Central Valley is now largely confined to low-lying rivers, most of which experience regulated flow regimes to accommodate agricultural, municipal, and industrial water use throughout the year (Brown and Ford 2002; Marchetti and Moyle 2001). The upstream migratory corridor for spawning adult Chinook salmon typically includes the San Francisco Bay-Delta estuary, mainstem Sacramento or San Joaquin River, and one large tributary such as the Yuba River, Feather River, Mokelumne River, American River, and others (Santos et al. 2014). Extensive channelization has occurred throughout the migratory corridor as part of flood control infrastructure and prevailing land use. These, damming, and other practices have inhibited natural flood regimes and floodplain connectivity in larger Central Valley rivers (Mount 1995). This has led to simplification of migratory habitat and losses of riparian canopy cover and instream wood (Gorman and Karr 1978; Simon and Rinaldi 2006). Additional stresses imposed on adult salmon migrating upstream in this region include recreational fishing, poaching, hydroacoustic impacts from in-water construction, and elevated water temperatures (Campbell and Moyle 1992; Stadler and Woodbury 2009; Strange 2010).

Central Valley rivers are highly managed through controlled releases of water from reservoirs on most major tributaries in the Sacramento and San Joaquin basins. Rivers typically experience steady and consistent hydrologic regimes that are highly altered relative to more episodic historical conditions (Brown and Bauer 2009). Although the system functions in an altered state compared to historical conditions, efforts have been underway in recent decades to integrate environmental flow management into release schedules (Jager and Rose 2003; Moyle et al. 1998).

1.2 | Study Purpose and Scientific Questions

This study investigated the influence of micro-scale hydraulic conditions at a regulated river confluence on routing pathways of Chinook salmon migrating to spawning grounds or a natal hatchery facility. Baldes and Vincent (1969) define microhabitat scale as "the physical conditions immediately surrounding an animal at a given time and place". Herein, we focus on the effects of hydrologic conditions that may be encountered by California Central Valley fall-run Chinook salmon during a drought year where minimum base flows are maintained in large, regulated rivers that provide water for a variety of agricultural, municipal, and industrial stakeholders (Herbold et al. 2018). This study addressed two questions: (1) Do magnitudes of discharge in each river at a confluence (and resulting combined discharge) influence availability of preferred hydraulic microhabitats in one river versus the other? (2) Does the ratio of discharge magnitudes influence availability of preferred hydraulic microhabitats in one river versus the other? The experimental design concept is discussed further below and graphically depicted in Figure 1.

2 | Methods

2.1 | Study Area

This study investigated the immediate confluence of the lower Feather River (LFR) and lower Yuba River (LYR), located in northeastern California in the northeastern portion of the

TABLE 1 | Summary of habitat suitability criteria found in previous assessments for migrating adult Chinook salmon. Curve type refers to the method of reporting habitat suitability. "% utilization" refers to numbers of fish detections corresponding to binned microhabitat conditions for depth or velocity. "Preference" is computed using % utilization and corrects for the amount of each habitat bin class available in the survey area.

	Burger et al. (1983)	Wampler (1986)	Aceituno (1990)
Location	Kenai River, AK	Wind River, WA	Stanislaus River, CA
Chinook salmon phenotype	Summer-run	Spring-run	Fall-run
Water temperature range during sampling (°C)	4.4–13.9	10.0–17.8	not reported
Survey method	Radio telemetry	Snorkel	Snorkel
Peak velocity (m/s)	0.8	1.1	0.4
Velocity range sampled (m/s)	0–1.7	0–1.7	0–1.5
Peak depth (m)	2.3	4.5	0.6–1.1
Depth range sampled (m)	0–3.9	0.3–4.6	0–1.5
Curve type (% Utilization vs. Preference)	% Utilization	Preference	Preference

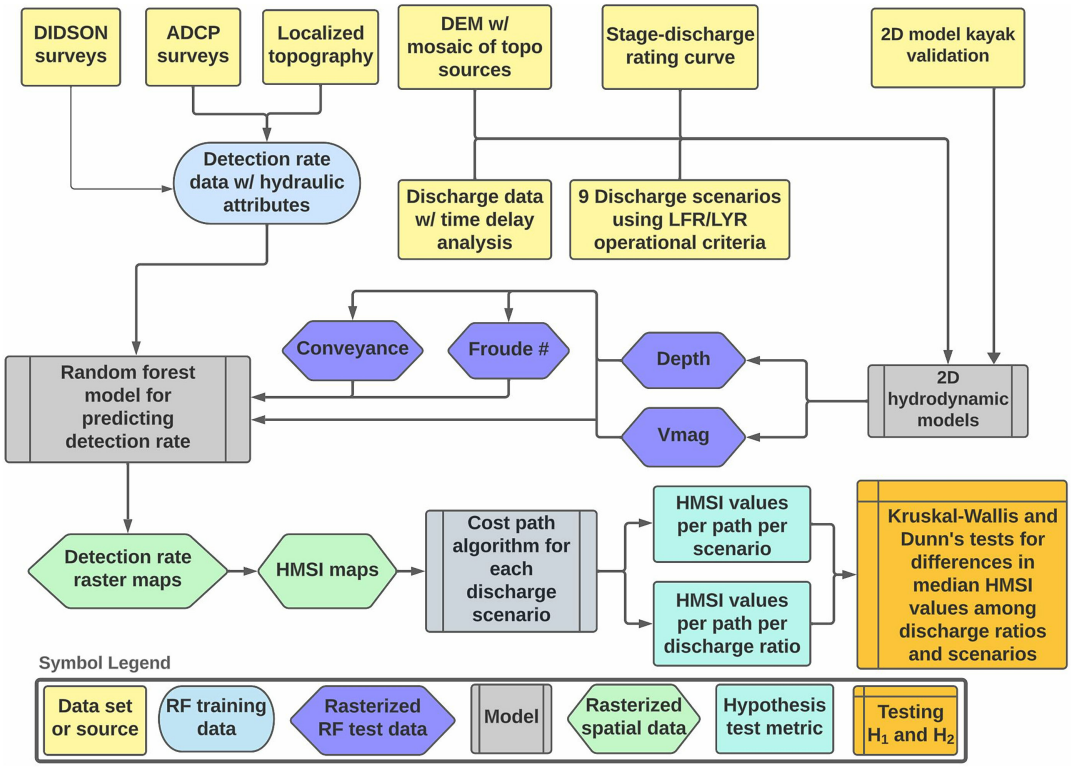

FIGURE 1 | Conceptual flow chart describing our study design and methods.

California Central Valley (Figure 2). Specifically, the study area as well as the modelling domain includes ~1.42 km of the LFR and 0.85 km of the LYR upstream of the confluence and 1.13 km of the LFR downstream of the confluence (Figure 3). Upstream of the LFR and LYR, the Feather River drainage area is 10,885 km^2. The LFR begins at the base of Oroville Dam, extending 117 km to its confluence with the Sacramento River. The CA Department of Water Resources filed a request with the Federal Energy Regulatory Commission to renew the dam's operational licence in 2005. This resulted in a request for a biological consultation under the federal Endangered Species Act with the National Marine Fisheries Service, which issued a Biological Opinion for the dam relicensing in 2016 (National Marine Fisheries Service 2016). Following a spillway collapse in 2017 that resulted in mobilization and downstream aggradation of approximately 1 million tons of debris from Lake Oroville, licence renewal is still pending (Nalin and Kotulla 2018, Federal Energy Regulatory Commission 2022). The 2016 Biological Opinion set forth operational criteria that would minimize take of Endangered Species Act-listed species, including minimum baseflow criteria. Because this study focuses on the Central Valley fall-run Chinook phenotype, we selected LFR baseflow criteria for October through February where the bulk of migratory activity for this population occurs. During this period, in years where the LFR receives >55% of unimpaired runoff from the Feather catchment, the minimum baseflow for the river is 48.13 m^3/s. In years where the LFR receives <55% of unimpaired runoff, the minimum baseflow is 33.97 m^3/s.

The Yuba drainage area is 3480 km^2. The LYR begins at the base of Englebright Dam, extending 37.1 km to its confluence with the LFR. In 2008, the California State Water Resources Control Board approved a comprehensive interagency program that would protect and enhance LYR aquatic and riparian habitat. The program is called the Lower Yuba River Accord and is managed by the Yuba Accord River Management Team (YARMT 2013). Minimum baseflow criteria set forth for Yuba Water Agency operations to support native fish habitat is based on upstream reservoir storage volume in Englebright Lake. For the purposes of our study, we focus on criteria during October where minimum baseflows range from 14.16 m^3/s in a very wet "schedule 1" year (annual reservoir storage of 7.08×10^8 m^3) to 9.91 m^3/s in a critically dry "schedule 6" year (annual reservoir storage of 2.86×10^8 m^3). After findings by YARMT indicated rates of non-natal adult Chinook salmon straying into the LYR were likely influenced by flow conditions (72% of population escapement variation in the LYR were attributed to discharge magnitude and temperature), the National Marine Fisheries Service's California Central Valley salmonid recovery plan included a recovery action to "evaluate whether salmonid straying between the Feather and Yuba rivers can be minimized through flow management" (YARMT 2013; National Marine Fisheries Service 2014).

2.2 | Experimental Design

Previously, Luis and Pasternack (2023) observed and characterized microhabitat preference and micro-scale migratory swimming behaviour responses to the following hydraulic variables: depth, velocity, conveyance, and Froude number. In this study, we use a combination of 2D hydrodynamic models, a random forest machine learning algorithm, and a nearest neighbour cost path movement algorithm to simulate migratory movements past a confluence in response to these four hydraulic variables under a

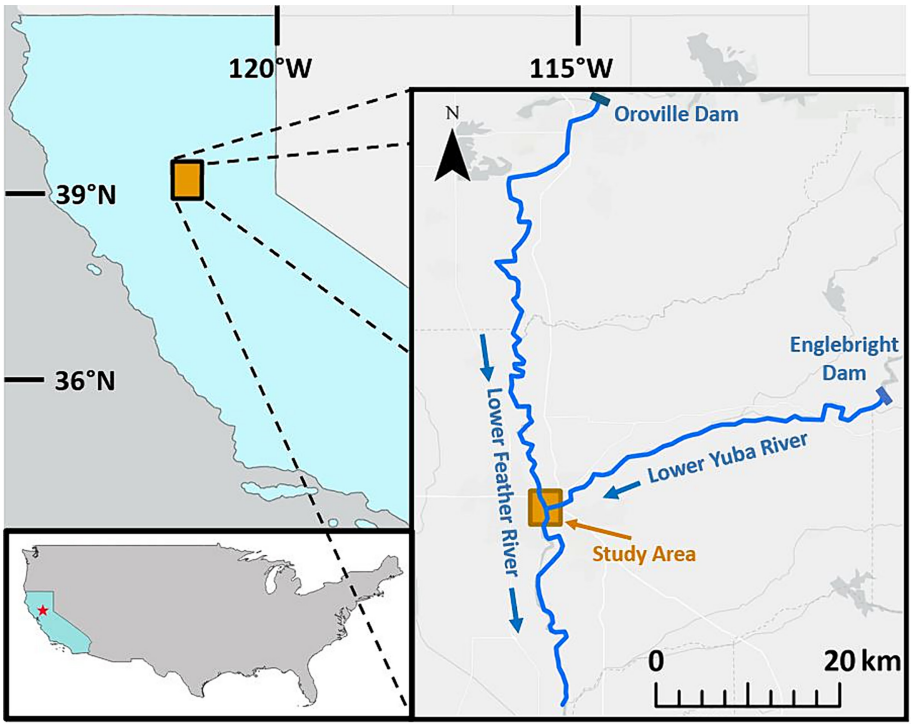

FIGURE 2 | Location of the study area. The state of California is shaded in blue in the main panel with an inset describing the location within the continental United States. The inset identifies the lower Feather River, lower Yuba River, and the dams that create total fish passage barriers upstream of the study area. Blue arrows indicate flow direction. Base map image sources: ESRI, HERE, Garmin, FAO, NOAA, USGS, © OpenStreetMap contributors, and the GIS user community.

suite of drought-focused discharge scenarios (Figure 1). The nine discharge scenarios are shown in Table 2, including individual discharge magnitudes and citing the regulatory context from which they are derived. Scenarios 1–4 explore minimum baseflow conditions in the LFR and LYR under both wet and dry water year types. These first four scenarios result in three different ratios of discharge magnitude, shown in Table 2. Scenarios five and six use a 1:1 discharge ratio, using both wet and dry minimum baseflow criteria for the LFR (minimum LYR baseflows cannot legally occur in the LFR). Scenarios 7–9 use the same three discharge ratios found in scenarios 1–4, but instead use the dry-type LFR baseflow as the lower value (33.97 m^3/s).

2D hydrodynamic models were run for these nine scenarios and output rasters for depth and velocity magnitude were produced; rasters for conveyance and Froude number were derived from these. Using cell values in the four hydraulic rasters for each scenario, a random forest model was used to generate spatially explicit predictions of detection rate; trained using the detection data from our previous study (Luis and Pasternack 2023). Random forest models have been shown to out-perform other multivariate statistical approaches using large data sets and have been applied in other 2D hydraulic modelling contexts (Fox et al. 2017; Hengl et al. 2018; Hosseiny et al. 2020). We then scaled the range of all detection rate values predicted among modelled scenarios to create a hydraulic microhabitat selectivity index (HMSI) between zero (least preferred) to one (most preferred). HMSI is representative of migratory habitat quality as a function of preferred hydraulic conditions. A cost path analysis was then performed to generate optimal upstream paths (seeking out the highest HMSI values along each path) from 10 laterally distributed starting positions across the downstream flow boundary, proceeding through the study area. This resulted in 10 cost paths for each of the nine scenarios.

Our study was designed to test two hypotheses. $\mathbf{H_1}$: the magnitudes of discharge in each river at the confluence (and resulting combined discharge) influence median HMSI values encountered among the 10 optimal migratory pathways per discharge scenario. $\mathbf{H_2}$: the ratio of discharge magnitudes influences median HMSI values encountered among the 10 optimal migratory pathways per discharge scenario. Null hypotheses state that there is no difference in median HMSI values encountered in cost paths among discharge scenarios or discharge ratios, respectively. The term "optimal" refers to the pathway derived by the cost path algorithm, seeking out the highest HMSI value in a nearest neighbour cell search. A Kruskal–Wallis test by ranks was used to test for statistically significant differences in median HMSI values among (1) nine discharge scenarios, and (2) ratios of discharge magnitude. Dunn's test for multiple comparisons was used to test for significant pairwise differences among the nine discharge scenarios and ratios of discharge magnitude to determine which scenario and ratio had the greatest effect among all examined. Not only were we interested in migratory routing at the confluence but also strength of influence of hydraulic microhabitats, indicated by the HMSI variable.

2.3 | Habitat Selection Data

In 2019, surveys of migratory habitat selection for adult fall-run Chinook salmon were conducted in the study area using

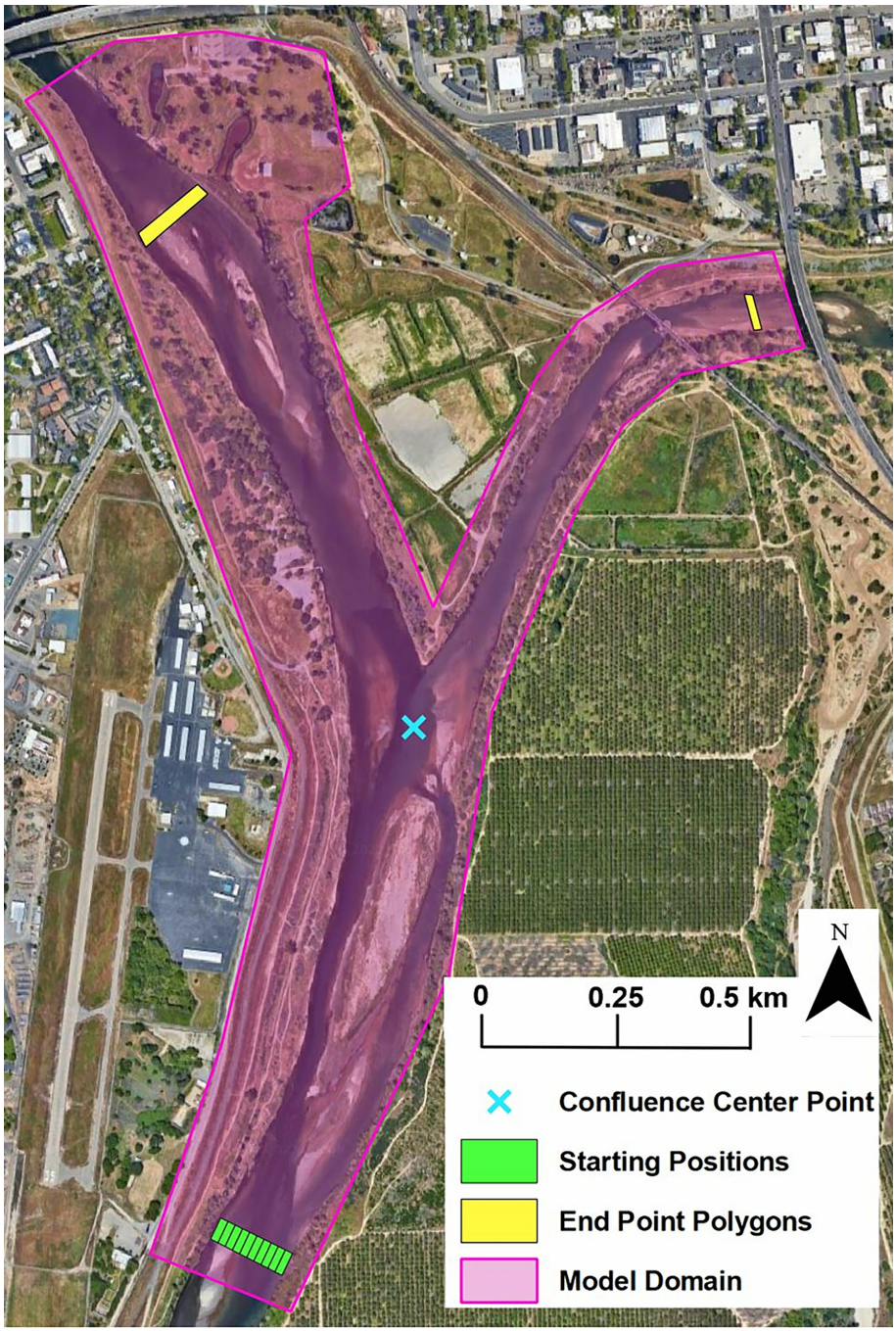

FIGURE 3 | Map of the study area including the extent of the model domain, start and end points for the cost path analysis, and the centre point used to establish starting and end point positions.

dual-frequency identification sonars (DIDSON; see Luis and Pasternack 2023). The DIDSON is a multibeam imaging sonar that can be used to render acoustic returns in a video format, allowing for underwater observation of fish behaviour (Belcher, Matsuyama, and Trimble 2001; Belcher, Hanot, and Burch 2002; Moursund, Carlson, and Peters 2003). The 2019 surveys occurred during two, 4-day periods in September and October, capturing two different discharge ratios between the LFR and LYR (8.66 and 4.02, respectively), resulting in different spatial distributions of depths and velocities throughout the study area. These sampling periods were selected based on their correspondence with the California Central Valley fall-run Chinook salmon spawning migration as well as known operational criteria at upstream dams. In 2019, the Feather River Hatchery accounted for 43.6% of hatchery-origin Chinook collected in the Sacramento and San Joaquin basins during the fall-run migration window. The hatchery is located ~ 61.9 RKM upstream of the LFR-LYR confluence. That year, 27,103 Chinook salmon returned to the hatchery with 51,967 in-river returns, totalling 79,070 fish (California Department of Fish and Wildlife [CDFW] 2022). Naturally spawning populations of spring- and fall-run Chinook persist in the LYR with no hatchery production in that river. In 2019, the LYR experienced 3446 in-river returns (CDFW 2022).

TABLE 2 | Discharge magnitudes and ratios for the nine modelled discharge scenarios used in this study. Regulatory context is cited for LFR and LYR baseflow criteria.

			LFR	
			< 55% unimpaired runoff (National Marine Fisheries Service 2016)	**> 55% unimpaired runoff (National Marine Fisheries Service 2016)**
			33.98 m^3/s	**48.14 m^3/s**
LYR	Schedule 6 (YARMT 2013)	9.91 m^3/s	Scenario 1 (3.4:1)	Scenario 2 (4.9:1)
	Schedule 1 (YARMT 2013)	14.16 m^3/s	Scenario 3 (2.4:1)	Scenario 4 (3.4:1)
	1:1 Ratio	33.98 m^3/s	Scenario 5 (1:1)	
		48.14 m^3/s		Scenario 6 (1:1)
	Inverse Ratios	81.55 m^3/s	Scenario 7 (1:2.4)	
		115.53 m^3/s	Scenario 8 (1:3.4)	
		166.50 m^3/s	Scenario 9 (1:4.9)	

Sampling occurred among 12 DIDSON deployment sites, capturing a representative range of depth and velocity occurring throughout the site, both above and below the confluence. A multiple regression analysis investigated potential predictive variables with detection rate (# individuals/m^3/s) as a response variable. Four hydraulic variables are included as attributes of detection rate (depth, velocity magnitude, conveyance, and Froude number). Depths for each DIDSON deployment were derived from the 2019 bathy-topographic surveys described below. Velocity magnitudes were computed from acoustic doppler current profiler surveys conducted in conjunction with the DIDSON surveys. Conveyance is defined as follows:

$$\overline{C} = \overline{u} * \overline{d} \quad (1)$$

where u is mean velocity magnitude in m/s and d is mean depth in m. C results in units of m^2/s and can be interpreted as the discharge per unit width of the wetted channel. It represents the local volumetric flow, which a fish inhabits at a given point in the wetted channel, and has been used in similar applications for assessing habitat suitability (Kammel et al. 2016; Moniz et al. 2019). Froude number is dimensionless and describes the ratio of inertial forces to gravitational forces in flow. It has also been used in other investigations into salmonid habitat suitability (Ayllón et al. 2009; Lamouroux and Souchon 2002; Persinger, Orth, and Averett 2011):

$$\overline{Fr} = \frac{\overline{u}}{\sqrt{g * \overline{d}}} \quad (2)$$

where u is the mean velocity magnitude at each site in m/s, g is the gravitational acceleration constant in m/s^2, and d is the mean depth at each site in m.

This study utilizes detection rate data and corresponding hydraulic predictors found by Luis and Pasternack (2023) to address the new, difference scientific questions posed herein.

2.4 | Topo-Bathymetric Surveying and DEM Construction

A digital elevation model (DEM) was created for the study area using several sources of topo-bathymetric point data (Figure S1 in supplementary materials). In 2019, bathymetric surveys were conducted using a boat mounted Hydrolite single beam echosounder (minimum depth of 0.3 m; depth accuracy of 1 cm; sampling frequency of 200 Hz; Seafloor Systems, Inc.) in sync with a Trimble R8 real-time kinematic GPS (horizontal and vertical accuracies of ~1–2 and 2–4 cm, respectively) receiving ground-based corrections on the fly at 1 Hz. Cross-sectional transects were mapped approximately one channel width apart. At the locations of DIDSON data collection, multiple cross-sections were performed with very close longitudinal spacing to ensure the most detail where the most data were collected. In addition, 8–12 longitudinal transects were surveyed down the length of the study area, because the primary topographic variability on the riverbed was longitudinal, not cross-sectional. Taken together, longitudinal and lateral surveys produced good coverage relative to the relatively gentle morphological structure present in this size of channel. The large island at the centre of the confluence contained some complex topography, and in January 2020, bare-earth topography was collected there using a Trimble R8 RTK GPS. To map riverbanks and islands just beyond the wetted area and water surface elevations needed in this study, a very small clip of pre-existing near-infrared and green LiDAR data was used, accounting for 8.7% of largest wetted area among hydraulic model outputs. It had been collected in 2017 by Yuba Water Agency and processed by our group to obtain a 0.9144 m (i.e., 3-ft) raster (Silva and Pasternack 2018). Processed LiDAR points within the clip were incorporated into the DEM. Counting all points in the largest wetted area domain, the overall DEM point density was 4.55/3 m^2.

All topo-bathymetric point data were processed to generate a DEM using ESRI ArcGIS software and the four iterative stages described by French and Clifford (2000): interpolation,

visualization, editing, and augmentation. Erroneous bathytopographic data points were identified and manually removed. Augmented points were also added manually to conserve known contours in the DEM and avoid any artefacts in the DEM that might occur from surface interpolation. A triangulated irregular network was generated from the final set of bed elevation points, and this was converted to a 3-m resolution raster based on overall point density and computational efficiency in the subsequent hydrodynamic modelling step. A smoothing algorithm using nearest neighbour cell averaging was applied to areas in the final DEM expected to be wetted in our discharge scenarios (bed elevations < 13.4 m) to further minimize surface interpolation artefacts.

2.5 | 2D Hydrodynamic Models and Model Validation

The 2D hydrodynamic model TUFLOW HPC© (Build 2018-03-AE; BMT Commercial Australia Pty Ltd) was used to simulate steady flow through the study area under the nine discharge scenarios shown in Table 2. TUFLOW HPC generates time- and depth-averaged gridded solutions of open channel hydraulics by solving the 2D shallow water fluid dynamics equations (mass and momentum consideration) that include fixed initial conditions such as discharge and water surface elevation, as well as fixed parameters of the model domain such as eddy viscosity coefficients and roughness coefficients (n). A gridded Cartesian computational mesh also provides better computational efficiency compared to an unstructured mesh, and is well-suited for this application due to the relatively simple channel geometry in our study area (Kim et al. 2014; Liu 2014). Data outputs of the model include rasters of depth, water surface elevation (WSE), velocity magnitude, and bed shear stress. All output rasters were created at a 3-m^2 cell resolution; given baseflow river widths of ~ 70–280 m this size yields ~ 23–90 cells across, which is plenty to resolve lateral changes in hydraulics.

The Smagorinsky formulation for eddy viscosity was used to account for momentum diffusion via turbulence in the model's momentum equations (BMT Commercial Australia Pty Ltd 2018). This equation requires parameters for both a constant coefficient and an initial Smagorinsky coefficient that is then updated on a cell-by-cell basis; we used 0.4 and 0.5, respectively.

TUFLOW HPC also requires several geospatial data layers as inputs to define boundary conditions for the model. The first is a topographic layer in which we used the final DEM raster described above. The second is a polygon shapefile that defines the Manning's n coefficient(s) being used for roughness. Because our study area is dominated by sand-sized substrate with gentle bedforms and intermittent bank vegetation, we used a uniform Manning's n value of 0.03 in all model runs in this study (Arcement and Schneider 1989; Limerinos 1970). Finally, cross-sectional polygons defining the upstream flow boundary (or boundaries in our case) with a corresponding discharge magnitude, as well as the downstream boundary with corresponding cross-sectional WSE. Figure S2 in supplementary materials shows the second order polynomial stage-discharge rating curve that was generated for our study area. WSEs were measured using a Trimble R8 RTK GPS near the downstream boundary of the study area under various discharge conditions from 2017 to 2019 to develop this curve (Figure 3). The curve was then used to interpolate WSEs that correspond to our modelled discharge scenarios. Discharge data was obtained from the California Department of Water Resources' Data Exchange Centre (CDWR 2023).

This study used the 2D model water velocity validation method of Barker et al. (2018). This approach is a variation of large-scale particle image velocimetry (e.g., Dramais et al. 2011). While this approach yields less accurate individual point velocity values than point-scale velocity instruments (e.g., acoustic doppler, electromagnetic, and propeller velocimeters), Barker et al. (2018) found it significantly outperformed model validation with those traditional tools for four reasons: (i) ability to observe velocity in locations that cannot be waded (i.e., too fast and/or too deep) and locations where a boat cannot hold position; (ii) better representation of the full range of velocities present, (iii) ability to collect velocity direction data, and (iv) collection of so much more data that model performance metrics have far higher accuracy and statistical significance.

On a windless day, a kayaker kept their boat moving exactly at the speed and direction of the water around it using floating debris as a visual aid. A Trimble R8 RTK GPS tracked kayak position at 1 Hz. Distance travelled per second was computed as a surface velocity and this value was assigned to the midpoint position of each measurement. Based on visual site reconnaissance, it was possible to map what appeared to be the full range of velocity for enough area to test model performance thoroughly. In addition to obtaining observed surface velocities, the method of Barker et al. (2018) was used to find a depth-average velocity constant of 0.63 and apply this to the observed data to obtain field-estimated depth-average velocities. Both the observed surface values and the estimated depth-averaged values were compared to depth-average model velocities at the same coordinates for the same steady flow regime that occurred during the day of the kayak survey (Figure 4).

2.6 | Random Forest Model

We utilized a random forest model to produce spatially explicitly estimates of detection rate throughout the wetted portion of the study area. A random forest model is a commonly used non-parametric machine learning algorithm that uses a classification and regression tree technique combined with a bootstrapping component to make robust predictions on a test data set using a training data set. Randomly selected values for a predictor variable (a fixed value for continuous data or a single class for categorical data) form nodes along a decision tree to make a prediction of a response variable value. Homogeneity is maximized within nodes and heterogeneity is maximized between nodes (Breiman 2001; Cutler et al. 2007).

In a random forest process, a user-defined number of trees are grown using random samples of the training data, with predictor values forming nodes along each tree. These trees are used to make predictions for out-of-bag (OOB) data (not included in the bootstrapped data set in each iteration). This feature of the

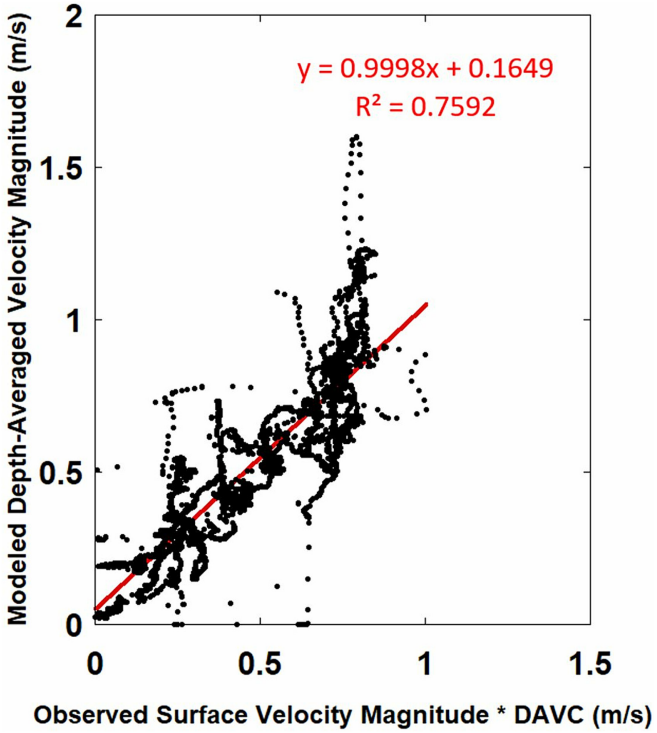

FIGURE 4 | Results of the kayak velocity validation survey. This plot compares the observed surface velocities multiplied by the depth-averaged velocity constant (DAVC) to the modelled depth-averaged velocity magnitude values from the TUFLOW model outputs to assess model accuracy and performance.

random forest process eliminates the need for an additional cross-validation step to evaluate model performance (Cutler et al. 2007; Segal 2004). Errors and accuracies of modelled predictions are averaged across the forest using these repeated OOB predictions. As a result, additional cross-validation to evaluate model performance is not necessary as this is a built-in feature of the random forest process (Cutler et al. 2007; Segal 2004). The bootstrapping component is also useful in that it avoids issues of model overfitting, which can be a concern in other statistical modelling approaches (Williams 2011).

The R package *randomForest* (Breiman 2001; Liaw and Wiener 2002; R Core Team 2023) was used to produce spatially-explicit predictions of detection rate. Modelling was performed with this package for each of the nine discharge scenarios using the four hydraulic variables from the 2019 DIDSON sampling campaign (depth, velocity magnitude, conveyance, and Froude number) to train the model. We utilized an approach for model calibration similar to van Poorten, Cox, and Cooper (2013). Parameters for node size (*nodesize*) and number of variables tested per node (*mtry*) were systematically tuned in preliminary trials to achieve the lowest value for residual mean squared error and holding the number of trees (*ntree*) at 250. To ensure stable predictions and stability of mean error values across the forest, the final model was run with 1000 trees. Final model parameters were: $nodesize = 4$, $mtry = 1$, $ntree = 1000$. Spatially explicit predictions of detection rate within the model domain were made using spatially explicit values for the four hydraulic variables, derived from the 2D hydraulic model outputs for depth and velocity magnitude for each of the nine discharge scenarios.

2.7 | Cost Path Analysis

The cost path algorithm in ESRI's ArcGIS Pro was used to simulate upstream migratory movement of adult Chinook salmon through the model domain. We created the HMSI variable to describe degree of preference for a given cell in the domain. The HMSI is scaled from zero to one, using the highest (equal to 1) and lowest (equal to 0) predicted values of detection rate among the nine discharge scenarios via the random forest's predictive output maps. Spatially explicit detection rates were converted to HMSI values and HMSI maps were generated by creating triangulated irregular networks from TUFLOW grid points and converting those to 3x3 m^2 rasters. Because HMSI maps were derived from TUFLOW outputs, HMSI maps span the wetted area for each discharge scenario.

The cost path algorithm uses an iterative nearest neighbour search process given a user-specified starting location to progress through a raster by identifying the "lowest cost" adjacent cell repeatedly until the path reaches a user-defined end point. In this study, the expected path is defined as following the maximum HMSI value available. Because the ArcGIS tool seeks minimum values, we created a "lowest cost" variable by simply computing 1-HMSI.

In this study of upstream migration, the starting point is at the downstream end of the confluence domain. To avoid bias resulting from specifying a single starting point, we generated 10 starting positions spaced evenly, extending laterally across the downstream boundary of the model domain (similar to the evenly-spaced starting positions in an agent-based model of juvenile eel migration by Benson et al. 2021; see Figure 3). Meanwhile, at the upstream end

of the study area, a fair cost basis was needed to compare the two rivers even though they were mapped to different upstream limits. A fair cost basis requires having equivalent channel lengths in each river upstream of the confluence. To obtain equal upstream channel lengths, a centre point at the confluence was approximated and used to generate equidistant upstream endpoints in LFR and LYR. Final distances for upstream and downstream of the confluence were 1080.2 and 1005.7 m, respectively.

Cost path parameters were set to produce single paths. Each of the nine discharge scenarios included 10 paths, with each path starting from a separate lateral position in the river, yielding 90 cost paths total. The 90 final cost paths were each stationed in 10-m intervals and the HMSI values at each point were added to the attribute table of the station point file for analysis. Given that paths had different lengths, number of points per path among all paths varied between 698 and 742 points.

2.8 | Data Analysis

HMSI values along the 10 cost paths in each discharge scenario were analysed to answer the two scientific questions (Section 1.2) by testing stated hypotheses (Section 2.3). To investigate whether discharge magnitude in each river drives the availability of high-value hydraulic microhabitats in one river versus the other, Kruskal–Wallis (KW) rank sum tests were used to test for differences in median HMSI values encountered in the 10 cost paths in each discharge scenario at 95% confidence (Kruskal and Wallis 1952; Ostertagová, Ostertag, and Kováč 2014). KW tests were also used to test median differences in HMSI values encountered in all cost paths associated with the four discharge ratios examined in this study (each of which included cost paths from two different discharge scenarios, or three different scenarios in the case of the 3.4:1 ratio, see Table 2). A Kolmogerov–Smirnov (KS) test for goodness of fit revealed that our data do not meet normality requirements for ANOVA, so the non-parametric KW test was used (Massey 1951). KW and KS tests were performed in R using the base library (R Core Team 2023).

A statistically significant KW test only indicates that one median value among samples is different from the others. To identify which discharge scenario and discharge magnitude ratio resulted in the greatest difference in median HMSI value from one or more of the others, Dunn's test for multiple comparisons using ranked sums was used to compute pairwise comparisons among all possible paired combinations of discharge scenarios and ratios of discharge magnitude (Dunn 1964). Dunn's test allows for examination of differenced in ranked median HMSI values among discharge scenarios and ratios to determine which is most different (i.e., results in the highest value habitat along simulated migratory pathways). Because the Dunn's test includes all possible pairwise comparisons among the nine discharge scenarios, there were 36 comparisons in all (i.e. reverse summation, $8+7+\ldots+1$). The R package *rstatix* was used to perform the Dunn's tests and because the test involves multiple pairwise comparisons, adjusted p values were computed using the Bonferroni method (Dunn 1961; Kassambara 2022).

3 | Results

3.1 | Hydraulic Model Performance

Model performance test metrics included coefficient of determination, bias (i.e., y-intercept distance from the origin), and mean signed and unsigned percent error (−4.11% and 28.27%, respectively; see Table S1 in supplementary materials for additional performance metrics). The coefficient of determination (r^2) between observed surface and modelled depth-averaged velocities was 0.76, which is above the typical level of model performance in the published literature.

3.2 | Random Forest Model Performance

The random forest model identified the relative importance of the predictors, but only explained 17.43% of variance (and mean sum of squared residuals equal to 0.0024). Reasons for this are discussed below. The variable importance plot in Figure 5 shows that conveyance was the most important variable in the random forest process while depth was the least important.

3.3 | Cost Path Results

Migratory routing at the LFR/LYR confluence, driven by hydraulic selectivity, resulted in different rivers being chosen upstream of the confluence among the nine discharge scenarios (Figures 6–8). Remarkably, river selection was completely independent of where across the river a fish starts the journey through the study area. In scenarios 1–6, all migratory paths

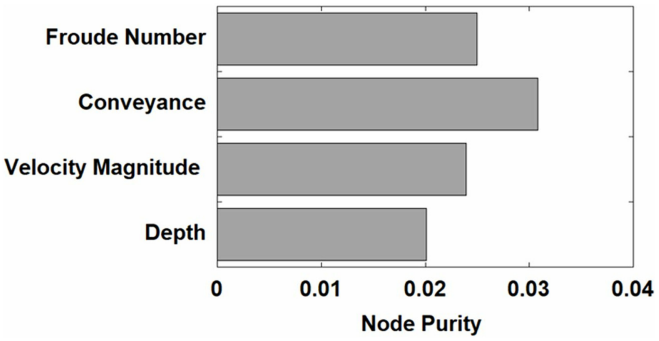

FIGURE 5 | Variable importance plot produced by the random forest model ranking the relative strength of each hydraulic predictor in predicting Chinook salmon detection rate.

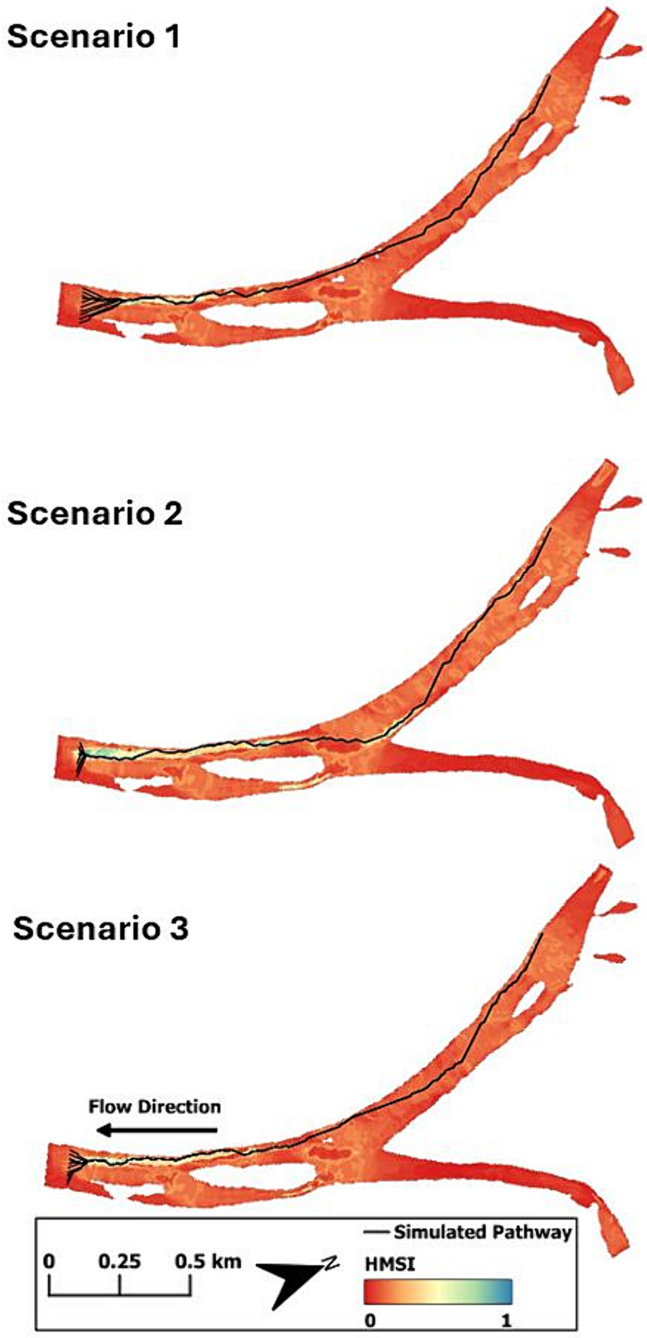

FIGURE 6 | HMSI raster maps and cost paths simulated for discharge scenarios 1–3. Raster layers have a 3 m cell resolution. Scenarios are numbered in the upper right corner of each panel.

converge quickly (within 0.25 km of the starting point). In scenarios 7–9, path convergence still occurs well before the confluence, but after a longer travel distance (0.6 km). This is due to the greater availability of high HMSI values distributed laterally, downstream of the confluence near the starting positions in those scenarios. The LFR is chosen in scenarios 1–5 which had mean HMSI values along pathways ranging from 0.25–0.37. In scenarios 6–9 where the LYR was chosen, mean HMSI values along pathways ranged from 0.41 to 0.51. This is a direct result of the spatial distribution of HMSI values throughout the model domain under each condition, but further testing was needed to determine the relative effects of discharge versus discharge ratio.

3.4 | Question 1: Discharge Effect

The KW test for differences in median HMSI values encountered in cost paths per discharge scenario was statistically significant at 95% confidence ($p < 0.01$), indicating at least one of the nine discharge scenarios resulted in greater value habitat overall compared to the others (Table 3 and Figure 9). Of the 36 pairwise tests, 31 (86%) had differences in ranked sums that were statistically significant. Table 4 includes paired differences in order of the sizes of difference between ranked sums. The greatest difference in median HMSI values was between scenario 1 (0.16) and scenario 9 (0.48; see Table 2 for scenario definitions).

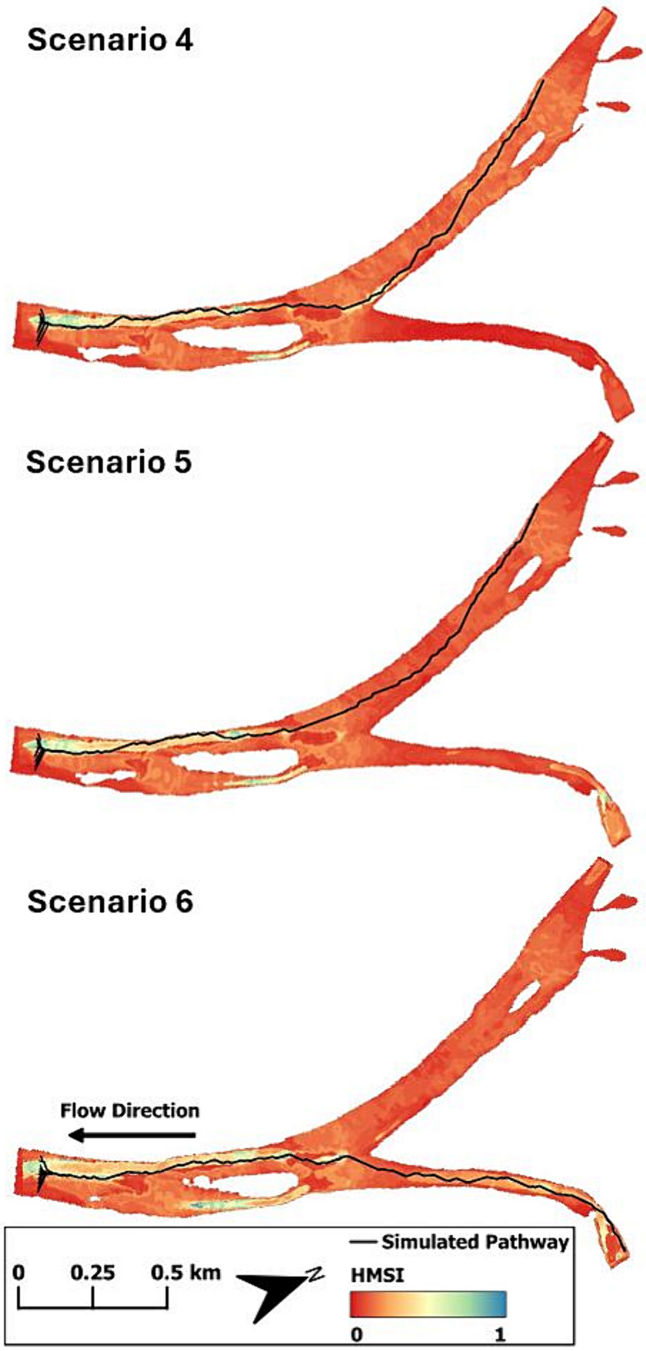

FIGURE 7 | HMSI raster maps and cost paths simulated for discharge scenarios 4–6. Raster layers have a 3 m cell resolution. Scenarios are numbered in the upper right corner of each panel.

Following this first pair of discharge scenarios are comparisons between scenario 1 and Scenarios 7 and 8; the second and third highest combined discharges that we examined.

3.5 | Question 2: Discharge Ratio Effect

As with the KW test for Question 1 regarding differences among discharge scenarios, the KW test for differences in median HMSI values encountered in cost paths per discharge ratio was statistically significant at 95% confidence ($p < 0.01$), indicating at least one of the four discharge ratios resulted in greater value habitat overall (Table 3 and Figure 10). The results of the Dunn's test shown in Table 5 (again, ordered in the table by the size of difference between ranked sums for each ratio) showed the highest difference in median HMSI values encountered between discharge ratios of 1:1 and 4.9:1. The relationship between HMSI and discharge ratio appears to be more complicated than

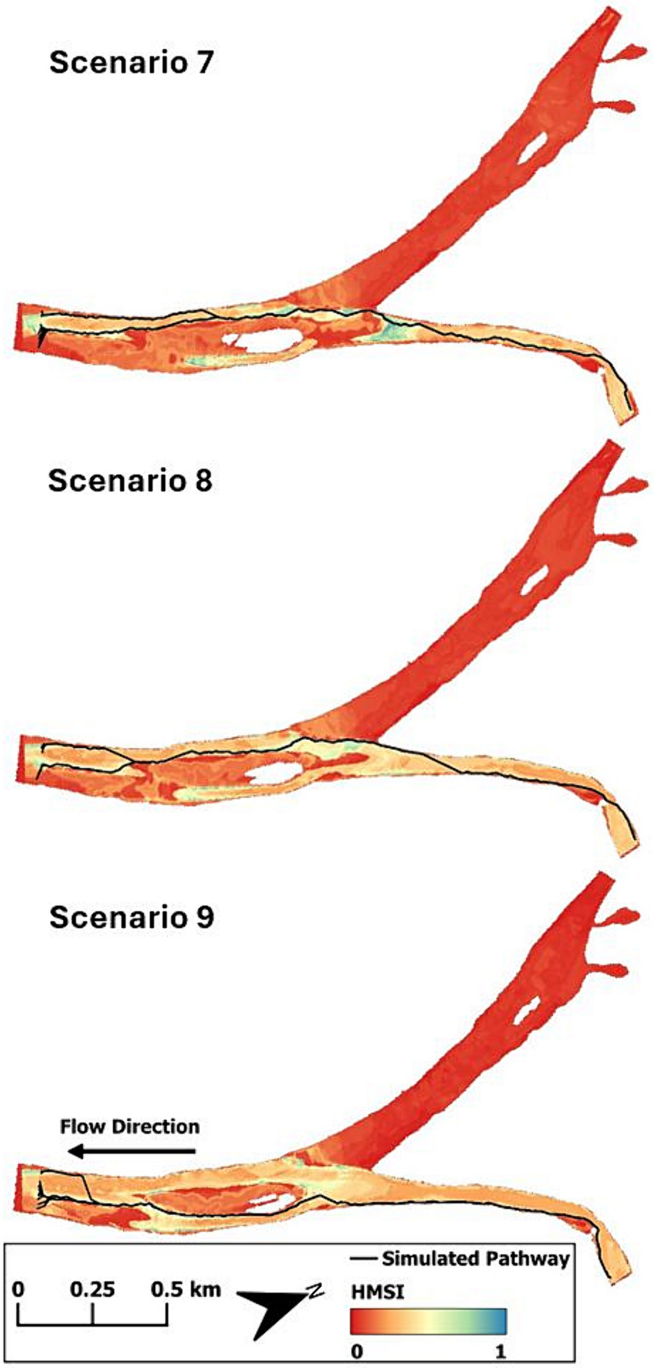

FIGURE 8 | HMSI raster maps and cost paths simulated for discharge scenarios 7–9. Raster layers have a 3 m cell resolution. Scenarios are numbered in the upper right corner of each panel.

TABLE 3 | Results of Kruskal–Wallis rank sum tests for differences in median HMSI values encountered among the nine discharge scenarios and four discharge ratios that occurred among the nine scenarios.

	DF	X^2_{KW}	p
Scenarios	8	15834.0	<0.001
Ratios	3	1648.7	<0.001

between HMSI and discharge magnitude, as the second greatest paired difference between ratios was 3.4:1 and 4.9:1. This is likely due to the 3.4:1 ratio appearing in three different discharge scenarios (as opposed to two, like the other three ratios examined), and so a greater sample of HMSI values represented by the 3.4:1 ratio. We did not find a directly proportional relationship between ratio and HMSI, indicating confluence discharges and combined discharge magnitude are more important predictors of habitat value within the confluence.

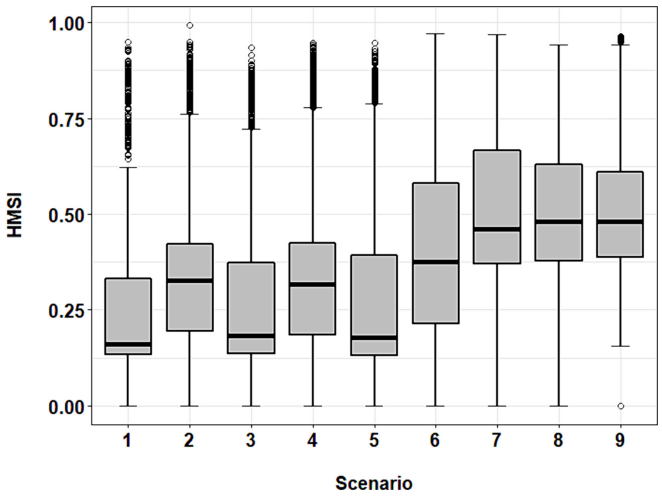

FIGURE 9 | Box and whisker plot indicating the median, quartiles, minima and maxima, and outliers (hollow circles) for HMSI values encountered along all cost paths in each scenario.

4 | Discussion

4.1 | High Uncertainty Found

Most physical habitat studies seek to predict usage of stationary ecological functions, such as holding, avoiding predators, prey capture, and spawning (Aceituno 1990; Bentley et al. 2014; Kammel et al. 2016; Magnhagen 1988; Nestler et al. 2019). In such stationary cases, studies have found a very tight coupling between physical habitat conditions and biological function (Moir et al. 2006; Moniz et al. 2019; Naman et al. 2019). In contrast, this study addressed the ecological function of fish migration in a sizeable river with dynamic swimming behaviour and instantaneous decision making at the microhabitat scale. The approach involved assessing typical hydraulic variables used in many aquatic physical micro-habitat studies, but these are only a small subset of many possible contributing factors. Specifically, fish migration is not only influenced by hydraulics around the fish, but also by other physico-chemical cues and behaviours such as olfactory homing and density-dependent behaviours (Berdahl et al. 2016; Berdahl, Westley, and Quinn 2017; null Dittman and Quinn 1996; Keefer and Caudill 2014; Unwin and Quinn 1993). Temperature is also known to influence migratory behaviour in adult salmonids (Goniea et al. 2006; Middleton et al. 2018; Salinger and Anderson 2006; Strange 2010). In this system, Luis and Pasternack (2023) found temperature to be an important variable along with conveyance in driving reach-scale habitat selection at the confluence of the LFR and LYR. However, we lacked the micro-scale spatial resolution in temperature data to incorporate it into this HMSI model and the random forest model predicting habitat selectivity contained significant uncertainty. This could potentially be done in the future using a forward-looking infrared raster data layer corresponding to modelled hydraulic scenarios.

Despite the high uncertainty, the results are meaningful and indicate predictive capability of the model because conveyance, velocity magnitude, and Froude number all have a velocity component, and ranked higher than depth in predictive power. For any given habitat cell in the model domain, the velocity magnitude value relative to the depth value provides key information for predicting HMSI. Thus, physical habitat is something that should be considered in assessing migration, but it is far from the only factor. By quantifying the degree of predictability of depth and velocity in migratory behaviour, this study adds important new understanding, even if that understanding is that these variables play a limited role.

4.2 | Migratory Routing in the LFR and LYR

The reason why depth and velocity should still be factored into river science and management, even if they only explain ~20% of behaviour, is that our results suggest migratory routing at the LFR/LYR confluence is partially driven by micro-scale hydraulic cues, as hydraulic selectivity is driven by discharge conditions. The simulations presented here are intended to complement the findings of Luis and Pasternack (2023) which showed hydraulic variables to be important factors in migratory microhabitat selection and rheotactic swimming behaviour. Based on DIDSON surveys conducted in 2019, it appears conveyance is the strongest hydraulic component of microhabitat selectivity.

Discharge magnitude was found to be an important driver of the amount and distribution of high-value hydraulic habitat. Results of the present study support previous patterns of adult Chinook escapement in this system, as the LYR has experienced elevated rates of strays in conditions where LYR discharge magnitude greatly outweighs that of LFR (observed as high as 6.5:1, see YARMT 2013). The conveyance variable has a velocity component, and thus is strongly driven by discharge magnitude as can be seen in scenarios 6–9 which had relatively high HMSI values compared to scenarios 1–5.

Discharge ratio was also found to be a statistically significant driver of hydraulic habitat distribution, though we expected to find a clearer relationship between discharge ratio and availability of high-value habitat at the confluence. Our investigation into this effect suggests discharge ratio may be an important

TABLE 4 | Results of Dunn's test for multiple comparisons among discharge scenarios. The pairwise comparisons of discharge scenarios are ordered by the absolute value of the difference in ranked sums between HMSI values along all cost paths per scenario, in each of the two scenarios analysed. Adjusted *p* values are shown using the Bonferroni method.

Scenario a	Scenario b	N_a	N_b	*rank a*	*rank b*	|*diff*|	*z*	*p*	p_{adj}
1	9	7017	7216	19161.38	44164.65	25003.27	79.72	**< 0.01**	**< 0.01**
1	8	7017	7244	19161.38	43803.82	24642.44	78.64	**< 0.01**	**< 0.01**
1	7	7017	7320	19161.38	43694.13	24532.75	78.49	**< 0.01**	**< 0.01**
3	9	7027	7216	22516.59	44164.65	21648.06	69.04	**< 0.01**	**< 0.01**
3	8	7027	7244	22516.59	43803.82	21287.23	67.96	**< 0.01**	**< 0.01**
5	9	7084	7216	22916.16	44164.65	21248.49	67.91	**< 0.01**	**< 0.01**
3	7	7027	7320	22516.59	43694.13	21177.54	67.78	**< 0.01**	**< 0.01**
5	8	7084	7244	22916.16	43803.82	20887.66	66.82	**< 0.01**	**< 0.01**
5	7	7084	7320	22916.16	43694.13	20777.97	66.64	**< 0.01**	**< 0.01**
1	6	7017	7339	19161.38	34378.43	15217.06	48.72	**< 0.01**	**< 0.01**
4	9	7275	7216	29735.39	44164.65	14429.26	46.42	**< 0.01**	**< 0.01**
4	8	7275	7244	29735.39	43803.82	14068.43	45.31	**< 0.01**	**< 0.01**
4	7	7275	7320	29735.39	43694.13	13958.74	45.07	**< 0.01**	**< 0.01**
2	9	7283	7216	30259.86	44164.65	13904.79	44.75	**< 0.01**	**< 0.01**
2	8	7283	7244	30259.86	43803.82	13543.95	43.63	**< 0.01**	**< 0.01**
2	7	7283	7320	30259.86	43694.13	13434.27	43.39	**< 0.01**	**< 0.01**
3	6	7027	7339	22516.59	34378.43	11861.85	37.99	**< 0.01**	**< 0.01**
5	6	7084	7339	22916.16	34378.43	11462.27	36.79	**< 0.01**	**< 0.01**
1	2	7017	7283	19161.38	30259.86	11098.48	35.47	**< 0.01**	**< 0.01**
1	4	7017	7275	19161.38	29735.39	10574.01	33.78	**< 0.01**	**< 0.01**
6	9	7339	7216	34378.43	44164.65	9786.22	31.55	**< 0.01**	**< 0.01**
6	8	7339	7244	34378.43	43803.82	9425.38	30.42	**< 0.01**	**< 0.01**
6	7	7339	7320	34378.43	43694.13	9315.70	30.15	**< 0.01**	**< 0.01**
2	3	7283	7027	30259.86	22516.59	7743.28	−24.75	**< 0.01**	**< 0.01**
2	5	7283	7084	30259.86	22916.16	7343.70	−23.52	**< 0.01**	**< 0.01**
3	4	7027	7275	22516.59	29735.39	7218.80	23.07	**< 0.01**	**< 0.01**
4	5	7275	7084	29735.39	22916.16	6819.23	−21.84	**< 0.01**	**< 0.01**
4	6	7275	7339	29735.39	34378.43	4643.04	15.00	**< 0.01**	**< 0.01**
2	6	7283	7339	30259.86	34378.43	4118.57	13.31	**< 0.01**	**< 0.01**
1	5	7017	7084	19161.38	22916.16	3754.78	11.92	**< 0.01**	**< 0.01**
1	3	7017	7027	19161.38	22516.59	3355.21	10.63	**< 0.01**	**< 0.01**
2	4	7283	7275	30259.86	29735.39	524.47	−1.69	0.09	1.00
7	9	7320	7216	43694.13	44164.65	470.52	1.52	0.13	1.00
3	5	7027	7084	22516.59	22916.16	399.57	1.27	0.20	1.00
8	9	7244	7216	43803.82	44164.65	360.84	1.16	0.25	1.00
7	8	7320	7244	43694.13	43803.82	109.68	0.35	0.72	1.00

N_a and N_b are the number of HMSI values along the cost path in each scenario, ranks *a* and *b* are the ranked sums per Dunn (1964),|*diff*|is the absolute value of difference in ranked sum between scenarios, *z* is the z statistic for testing significance at 95% confidence. p_{adj} is the adjusted *p* value using the Bonferroni method. Bolded *p* values are statistically significant.

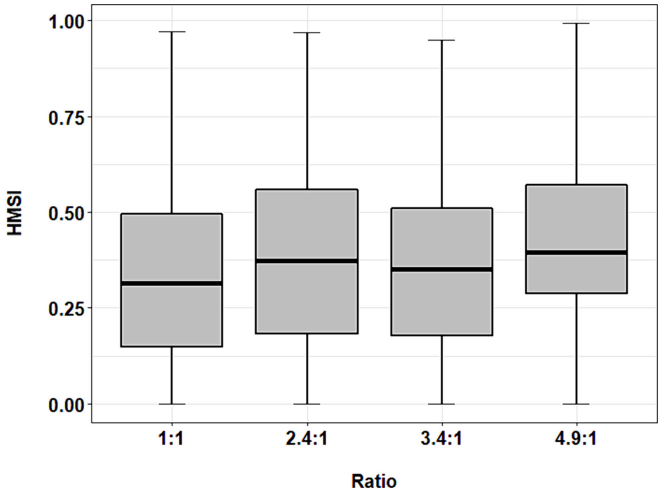

FIGURE 10 | Box and whisker plot indicating the median, quartiles, minima and maxima for HMSI values encountered along all cost paths corresponding to the four discharge ratios that occurred among the nine discharge scenarios.

TABLE 5 | Results of Dunn's test for multiple comparisons among flow ratios. The pairwise comparisons of discharge ratios are ordered by the absolute value of the difference in ranked sums between HMSI values along all cost paths per scenario, in each of the two scenarios analysed. Adjusted *p* values are shown using the Bonferroni method.

Ratio a	Ratio b	N_a	N_b	*rank a*	*rank b*	$\|diff\|$	*z*	*p*	p_{adj}
1:1	4.9:1	14,423	14,499	28748.62	37180.13	8431.51	38.32	**<0.001**	**<0.001**
3.4:1	4.9:1	21,536	14,499	31022.25	37180.13	6157.88	30.64	**<0.001**	**<0.001**
1:1	2.4:1	14,423	14,347	28748.62	33321.61	4572.98	20.73	**<0.001**	**<0.001**
2.4:1	4.9:1	14,347	14,499	33321.61	37180.13	3858.52	17.51	**<0.001**	**<0.001**
2.4:1	3.4:1	14,347	21,536	33321.61	31022.25	2299.36	−11.41	**<0.001**	**<0.001**
1:1	3.4:1	14,423	21,536	28748.62	31022.25	2273.63	11.30	**<0.001**	**<0.001**

N_a and N_b are the number of HMSI values along the cost path corresponding to each discharge ratio, ranks *a* and *b* are the ranked sums per Dunn (1964),$|diff|$is the absolute value of difference in ranked sum between discharge ratios, *z* is the z statistic for testing significance at 95% confidence. p_{adj} is the adjusted *p* value using the Bonferroni method. Bolded *p* values are statistically significant.

predictor of migratory routing within a certain range of discharge magnitude values. At a confluence, depending on the size of discharge ratios, a backwater effect may also occur in the river with a lower discharge, lowering velocities in that river upstream of the confluence and yielding lower HMSI values that might be attractive to migrating salmon.

An example of discharge ratio influencing migratory routing can be seen in Table 4 where scenarios 7–9 are highly influential, having the three greatest combined discharge magnitudes among our simulations when compared to scenario 1. The differences in ranked HMSI sums among scenarios 7–9 were markedly different, with the comparison between scenarios 9 and 1 having almost twice the difference compared to the comparison between scenarios 7 and 1. This can be seen graphically in Figure 8 where the LYR in scenario 9 has higher overall HMSI values along the cost paths when compared to scenario 7. Therefore, in the context of potential drought conditions at the LFR/LYR confluence, a situation with a high combined discharge occurring simultaneously with a high discharge ratio has the potential to greatly determine migratory routing via hydraulic habitat selectivity. Again, this is the situation that was observed in 2010 in this system that resulted in an acute pulse of LFR-origin fall-run Chinook salmon straying into LYR.

4.3 | Information Gaps and Future Modelling Applications

Even though adult salmon migration has been studied for decades in many different systems and species, researchers, managers, and policy makers still lack a cohesive, holistic quantitative model of the navigational cues for homing and upstream travel. To date, research has shown that this process is extremely complex, involving many different sensory inputs as well as endocrine responses in an individual fish. Our hope is that this modelling study provides some compelling evidence that micro-scale hydraulic cues also play a limited but important role, necessitating further research. For example, there should be observational and modelling efforts to unify olfactory responses, density-dependent behaviour, micro-scale hydraulic selectivity, innate exploratory behaviour, and responses to other habitat characteristics such as temperature, turbidity, pathogens, substrate, and channel complexity.

A good starting point would be a study that tracks both hydraulic habitat selectivity and fidelity to olfactory cues so that degree of influence of micro-scale habitat characteristics could be disentangled from olfactory homing mechanisms for a given species, population, and location. It is well understood that olfaction is a primary driver of homing and is likely the dominant driver of an individual's navigational choices (Cooper et al. 1976; A. H. Dittman, Quinn, and Nevitt 1996; A. D. Hasler and Scholz 1983; Ueda 2011), but there have also been multiple cases in which olfaction was shown to be compromised, such as hatchery-origin fish released away from their natal facility and denied the sequence of olfactory imprinting associated with outmigration (Huber et al. 2015; Jonsson, Jonsson, and Hansen 2003; Keefer and Caudill 2014; Murdoch, Tonseth, and Miller 2009; Sturrock et al. 2019). Exposure to waterborne pesticide compounds that are toxic to olfactory organs is another reason in which olfactory physiology may be compromised in adult salmon (Tierney et al. 2008, 2010). In these cases, hydraulic navigation cues may play a critical role in navigation in lieu of olfactory cues. The degree to which this occurs may also vary among species and migratory phenotypes. Bett and Hinch (2016) proposed a hierarchical navigation hypothesis based on existing empirical evidence that habitat selection in upstream migration occurs using a hierarchy of navigational cues with imprinted odours being the primary cue, conspecific odours being a secondary cue, and non-olfactory environmental factors as tertiary cues. Our intent was to provide some novel insight into how such non-olfactory cues may be incorporated in upstream navigation.

4.4 | Implications for Environmental Flow Management Strategies

Our findings highlight a broad need for future research and development of modelling tools that account for environmental navigational cues on homing and migration in adult salmon. With the exception of pulse attraction flows, research supporting flow regulation and watershed management strategies for salmon habitat functionality focuses on spawning, incubation, and juvenile rearing and outmigration (Harnish et al. 2014; Matella and Merenlender 2015; Schaller, Petrosky, and Tinus 2014; Zeug et al. 2014). Supporting these life stages is important for maintaining and improving population productivity and abundance for broader ecosystem support as well as fishery management. However, population attributes such as genetic structure, migration phenology, and spatial structure are conserved through successful adult migration and homing to natal streams (Narum et al. 2008; Powell and Campbell 2020; Vähä et al. 2007). In some cases, maintaining these attributes may be critically important for conservation efforts. For imperilled populations that experience high rates of straying, it may be prudent for water managers to consider developing and incorporating operational criteria into flow schedules that support successful homing by avoiding hydraulic conditions at key points along the migratory route that may encourage straying. Such criteria would take into consideration the escapement and spawn timing of an imperilled species, as well as an understanding of confluence hydrodynamics along their migratory pathway under ecologically, and operationally relevant discharge scenarios.

Acknowledgements

This project was financially supported by the Bob Wisecarver Memorial Scholarship awarded by the Diablo Valley Fly Fishermen; Small Projects Grant awarded by the Western Division of the American Fisheries Society; and Henry A. Jastro Graduate Research Award awarded by the University of California Davis. Student funding was also provided through the Chapter 33 Post 9/11 G.I. Bill through the U.S. Department of Veterans Affairs. This project was also supported by the USDA National Institute of Food and Agriculture, Hatch project number CA-D-LAW-7034-H.

Data Availability Statement

The data that support the findings of this study are available from the corresponding author upon reasonable request.

References

Aceituno, M. E. 1990. *Habitat Preference Criteria for Fall-Run Chinook Salmon Holding, Spawning, and Rearing in the Stanislaus River, California*. Sacramento, CA: U.S. Fish and Wildlife Service.

Acreman, M., J. Aldrick, C. Binnie, et al. 2009. "Environmental Flows From Dams: The Water Framework Directive." *Proceedings of the Institution of Civil Engineers: Engineering Sustainability* 162, no. 1: 13–22. https://doi.org/10.1680/ensu.2009.162.1.13.

Arcement, G. J., and V. R. Schneider. 1989. *Guide for Selecting Manning's Roughness Coefficients for Natural Channels and Flood Plains*. Federal Highway Administration: United States Geological Survey and the United States Department of Transportation.

Ayllón, D., A. Almodóvar, G. G. Nicola, and B. Elvira. 2009. "Interactive Effects of Cover and Hydraulics on Brown Trout Habitat Selection Patterns." *River Research and Applications* 25, no. 8: 1051–1065. https://doi.org/10.1002/rra.1215.

Baldes, R. J., and R. E. Vincent. 1969. "Physical Parameters of Microhabitats Occupied by Brown Trout in an Experimental Flume." *Transactions of the American Fisheries Society* 98, no. 2: 230–238. https://doi.org/10.1577/1548-8659(1969)98[230:PPOMOB]2.0.CO;2.

Barker, J. R., G. B. Pasternack, P. M. Bratovich, D. A. Massa, J. R. Wyrick, and T. R. Johnson. 2018. "Kayak Drifter Surface Velocity Observation for 2D Hydraulic Model Validation." *River Research and Applications* 34, no. 2: 124–134. https://doi.org/10.1002/rra.3238.

Belcher, E., W. Hanot, and J. Burch. 2002. "Dual-Frequency Identification Sonar (DIDSON)." In *Proceedings of the 2002 Interntional Symposium on Underwater Technology (Cat. No.02EX556)*, 187–192. Seattle, WA: IEEE. https://doi.org/10.1109/UT.2002.1002424.

Belcher, E., B. Matsuyama, and G. Trimble. 2001. "Object Identification With Acoustic Lenses. MTS/IEEE Oceans 2001. An Ocean Odyssey." In *Conference Proceedings (IEEE cat. No.01CH37295)*, vol. 1, 6–11. Seattle, WA: IEEE. https://doi.org/10.1109/OCEANS.2001.968656.

Benjankar, R., D. Tonina, J. A. McKean, M. M. Sohrabi, Q. Chen, and D. Vidergar. 2018. "Dam Operations may Improve Aquatic Habitat and Offset Negative Effects of Climate Change." *Journal of Environmental Management* 213: 126–134. https://doi.org/10.1016/j.jenvman.2018.02.066.

Benson, T., J. De Bie, J. Gaskell, et al. 2021. "Agent-Based Modelling of Juvenile Eel Migration via Selective Tidal Stream Transport." *Ecological Modelling* 443: 109448. https://doi.org/10.1016/j.ecolmodel.2021.109448.

Bentley, K. T., D. E. Schindler, T. J. Cline, et al. 2014. "Predator Avoidance During Reproduction: Diel Movements by Spawning Sockeye Salmon Between Stream and Lake Habitats." *Journal of Animal Ecology* 83, no. 6: 1478–1489. https://doi.org/10.1111/1365-2656.12223.

Berdahl, A., P. A. H. Westley, S. A. Levin, I. D. Couzin, and T. P. Quinn. 2016. "A Collective Navigation Hypothesis for Homeward Migration in Anadromous Salmonids." *Fish and Fisheries* 17, no. 2: 525–542. https://doi.org/10.1111/faf.12084.

Berdahl, A., P. A. H. Westley, and T. P. Quinn. 2017. "Social Interactions Shape the Timing of Spawning Migrations in an Anadromous Fish." *Animal Behaviour* 126: 221–229. https://doi.org/10.1016/j.anbehav.2017.01.020.

Bernazzani, P., B. A. Bradley, and J. J. Opperman. 2012. "Integrating Climate Change Into Habitat Conservation Plans Under the U.S. Endangered Species Act." *Environmental Management* 49, no. 6: 1103–1114. https://doi.org/10.1007/s00267-012-9853-2.

Best, J. L. 1986. "The Morphology of River Channel Confluences." *Progress in Physical Geography: Earth and Environment* 10, no. 2: 157–174. https://doi.org/10.1177/030913338601000201.

Best, J. L. 1988. "Sediment Transport and Bed Morphology at River Channel Confluences." *Sedimentology* 35, no. 3: 481–498. https://doi.org/10.1111/j.1365-3091.1988.tb00999.x.

Bett, N. N., and S. G. Hinch. 2016. "Olfactory Navigation During Spawning Migrations: A Review and Introduction of the Hierarchical Navigation Hypothesis: Olfactory Navigation During Spawning Migrations." *Biological Reviews* 91, no. 3: 728–759. https://doi.org/10.1111/brv.12191.

BMT Commercial Australia Pty Ltd. 2018. "TUFLOW User Manual—Build 2018-03-AE."

Boyer, C., A. G. Roy, and J. L. Best. 2006. "Dynamics of a River Channel Confluence With Discordant Beds: Flow Turbulence, Bed Load Sediment Transport, and Bed Morphology." *Journal of Geophysical Research* 111, no. F4: F04007. https://doi.org/10.1029/2005JF000458.

Breiman, L. 2001. "Random Forests." *Machine Learning* 45, no. 1: 5–32. https://doi.org/10.1023/A:1010933404324.

Brown, L. R., and M. L. Bauer. 2009. "Effects of Hydrologic Infrastructure on Flow Regimes of California's Central Valley Rivers: Implications for Fish Populations." *River Research and Applications* 26: 751–765. https://doi.org/10.1002/rra.1293.

Brown, L. R., and T. Ford. 2002. "Effects of Flow on the Fish Communities of a Regulated California River: Implications for Managing Native Fishes." *River Research and Applications* 18, no. 4: 331–342. https://doi.org/10.1002/rra.673.

Burger, C. V., D. B. Wangaard, R. L. Wilmot, and A. N. Palmisano. 1983. *Salmon Investigations in the Kenai River, AK, 1979–1981*. Anchorage, AK: National Fisheries Research Center, U.S. Fish and Wildlife Service.

California Department of Water Resources. 2023. *California Data Exchange Center [Computer Software]*. Sacramento, CA: State of California. http://cdec.water.ca.gov/index.html.

California Department of Fish and Wildlife (CDFW). 2022. "Fisheries Branch Anadromous Assessment – GrandTab." Annual Report.

Campbell, E. A., and P. B. Moyle. 1992. *Effects of Temperature, Flow, and Disturbance on Adult Spring-Run Chinook Salmon* (Technical Completion Report W-764). Davis, CA: University of California - Water Resources Center.

Caretta, M. A., A. Mukherji, M. Arfanuzzaman, et al. 2022. "Water (Chapter 4; Climate Change 2022: Impacts, Adaptation, and Vulnerability)." In *Contribution of Working Group II to the Sixth Assessment Report of the Intergovernmental Panel on Climate Change*, edited by H.-O. Pörtner, D. C. Roberts, M. Tignor, E. S. Poloczanska, K. Mintenbeck, A. Alegría, M. Craig, S. Langsdorf, S. Löschke, V. Möller, A. Okem, and B. Rama, 551–712. Cambridge, UK: Cambridge University Press. https://www.ipcc.ch/report/ar6/wg2/downloads/report/IPCC_AR6_WGII_FinalDraft_Chapter04.pdf.

Constantinescu, G., S. Miyawaki, B. Rhoads, and A. Sukhodolov. 2016. "Influence of Planform Geometry and Momentum Ratio on Thermal Mixing at a Stream Confluence With a Concordant Bed." *Environmental Fluid Mechanics* 16, no. 4: 845–873. https://doi.org/10.1007/s10652-016-9457-0.

Cook, B. I., J. S. Mankin, and K. J. Anchukaitis. 2018. "Climate Change and Drought: From Past to Future." *Current Climate Change Reports* 4, no. 2: 164–179. https://doi.org/10.1007/s40641-018-0093-2.

Cooper, J. C., A. T. Scholz, R. M. Horrall, A. D. Hasler, and D. M. Madison. 1976. "Experimental Confirmation of the Olfactory Hypothesis With Homing, Artificially Imprinted Coho Salmon (*Oncorhynchus kisutch*)." *Journal of the Fisheries Research Board of Canada* 33, no. 4: 703–710. https://doi.org/10.1139/f76-087.

Cutler, D. R., T. C. Edwards, K. H. Beard, et al. 2007. "Random Forests for Classification in Ecology." *Ecology* 88, no. 11: 2783–2792. https://doi.org/10.1890/07-0539.1.

Dahl, J., J. Dannewitz, L. Karlsson, E. Petersson, A. Löf, and B. Ragnarsson. 2004. "The Timing of Spawning Migration: Implications of Environmental Variation, Life History, and Sex." *Canadian Journal of Zoology* 82, no. 12: 1864–1870. https://doi.org/10.1139/z04-184.

Dai, A., T. Zhao, and J. Chen. 2018. "Climate Change and Drought: A Precipitation and Evaporation Perspective." *Current Climate Change Reports* 4, no. 3: 301–312. https://doi.org/10.1007/s40641-018-0101-6.

Di Baldassarre, G., F. Martinez, Z. Kalantari, and A. Viglione. 2017. "Drought and Flood in the Anthropocene: Feedback Mechanisms in Reservoir Operation." *Earth System Dynamics* 8, no. 1: 225–233. https://doi.org/10.5194/esd-8-225-2017.

Dittman, A. H., and T. P. Quinn. 1996. "Homing in Pacific Salmon: Mechanisms and Ecological Basis." *Journal of Experimental Biology* 199, no. Pt 1: 83–91.

Dittman, A. H., T. P. Quinn, and G. A. Nevitt. 1996. "Timing of Imprinting to Natural and Artificial Odors by Coho Salmon (*Oncorhynchus kisutch*)." *Canadian Journal of Fisheries and Aquatic Sciences* 53, no. 2: 434–442. https://doi.org/10.1139/f95-185.

Dramais, G., J. Le Coz, B. Camenen, and A. Hauet. 2011. "Advantages of a Mobile LSPIV Method for Measuring Flood Discharges and Improving Stage–Discharge Curves." *Journal of Hydro-Environment Research* 5, no. 4: 301–312. https://doi.org/10.1016/j.jher.2010.12.005.

Dunn, O. J. 1961. "Multiple Comparisons Among Means." *Journal of the American Statistical Association* 56, no. 293: 52–64. https://doi.org/10.1080/01621459.1961.10482090.

Dunn, O. J. 1964. "Multiple Comparisons Using Rank Sums." *Technometrics* 6, no. 3: 241–252. https://doi.org/10.1080/00401706.1964.10490181.

Federal Energy Regulatory Commission. 2022. "Pending License, Relicense, and Exemption Applications." https://cms.ferc.gov/licensing.

Fisher, A. C., W. Michael Hanemann, and A. G. Keeler. 1991. "Integrating Fishery and Water Resource Management: A Biological Model of a California Salmon Fishery." *Journal of Environmental Economics and Management* 20, no. 3: 234–261. https://doi.org/10.1016/0095-0696(91)90011-7.

Fox, E. W., R. A. Hill, S. G. Leibowitz, A. R. Olsen, D. J. Thornbrugh, and M. H. Weber. 2017. "Assessing the Accuracy and Stability of Variable Selection Methods for Random Forest Modeling in Ecology." *Environmental Monitoring and Assessment* 189, no. 7: 316. https://doi.org/10.1007/s10661-017-6025-0.

French, J. R., and N. J. Clifford. 2000. "Hydrodynamic Modelling as a Basis for Explaining Estuarine Environmental Dynamics: Some Computational and Methodological Issues." *Hydrological Processes* 14, no. 11–12: 2089–2108. https://doi.org/10.1002/1099-1085(20000815/30)14:11/12<2089::aid-hyp56>3.0.co;2-l.

Gaudet, J. M., and A. G. Roy. 1995. "Effect of Bed Morphology on Flow Mixing Length at River Confluences." *Nature* 373, no. 6510: 138–139. https://doi.org/10.1038/373138a0.

Goniea, T. M., M. L. Keefer, T. C. Bjornn, C. A. Peery, D. H. Bennett, and L. C. Stuehrenberg. 2006. "Behavioral Thermoregulation and Slowed Migration by Adult Fall Chinook Salmon in Response to High Columbia River Water Temperatures." *Transactions of the American Fisheries Society* 135, no. 2: 408–419. https://doi.org/10.1577/T04-113.1.

Good, T. P., T. J. Beechie, P. McElhany, M. M. McClure, and M. H. Ruckelshaus. 2007. "Recovery Planning for Endangered Species Act-Listed Pacific Salmon: Using Science to Inform Goals and Strategies." *Fisheries* 32, no. 9: 426–440. https://doi.org/10.1577/1548-8446(2007)32[426:RPFESL]2.0.CO;2.

Gorman, O. T., and J. R. Karr. 1978. "Habitat Structure and Stream Fish Communities." *Ecology* 59, no. 3: 507–515. https://doi.org/10.2307/1936581.

Gualtieri, C., M. Ianniruberto, N. Filizola, R. Santos, and T. Endreny. 2017. "Hydraulic Complexity at a Large River Confluence in the Amazon Basin." *Ecohydrology* 10, no. 7: e1863. https://doi.org/10.1002/eco.1863.

Harnish, R. A., R. Sharma, G. A. McMichael, R. B. Langshaw, and T. N. Pearsons. 2014. "Effect of Hydroelectric Dam Operations on the Freshwater Productivity of a Columbia River Fall Chinook Salmon Population." *Canadian Journal of Fisheries and Aquatic Sciences* 71, no. 4: 602–615. https://doi.org/10.1139/cjfas-2013-0276.

Hasler, A. D., and A. T. Scholz. 1983. *Olfactory Imprinting and Homing in Salmon: Investigations Into the Mechanism of the Imprinting Process*. Berlin (Heidelberger Platz), Germany: Springer.

Hasler, C. T., E. Guimond, B. Mossop, S. G. Hinch, and S. J. Cooke. 2014. "Effectiveness of Pulse Flows in a Regulated River for Inducing Upstream Movement of an Imperiled Stock of Chinook Salmon." *Aquatic Sciences* 76, no. 2: 231–241. https://doi.org/10.1007/s00027-013-0332-5.

He, M., J. Anderson, E. Lynn, and W. Arnold. 2021. "Projected Changes in Water Year Types and Hydrological Drought in California's Central Valley in the 21st Century." *Climate* 9, no. 2: 26. https://doi.org/10.3390/cli9020026.

Hengl, T., M. Nussbaum, M. N. Wright, G. B. M. Heuvelink, and B. Gräler. 2018. "Random Forest as a Generic Framework for Predictive Modeling of Spatial and Spatio-Temporal Variables." *PeerJ* 6: e5518. https://doi.org/10.7717/peerj.5518.

Herbold, B., S. M. Carlson, R. Henery, et al. 2018. "Managing for Salmon Resilience in California's Variable and Changing Climate." *San Francisco Estuary and Watershed Science* 16, no. 2: 1–23. https://doi.org/10.15447/sfews.2018v16iss2art3.

Hillman, M. 2009. "Integrating Knowledge: The Key Challenge for a New Paradigm in River Management: New Paradigm in River Management." *Geography Compass* 3, no. 6: 1988–2010. https://doi.org/10.1111/j.1749-8198.2009.00278.x.

Horne, A. C., J. A. Webb, M. J. Stewardson, B. Richter, and M. Acreman. 2017. *Water for the Environment: From Policy and Science to Implementation and Management*. London, UK: Academic Press, an imprint of Elsevier.

Hosseiny, H., F. Nazari, V. Smith, and C. Nataraj. 2020. "A Framework for Modeling Flood Depth Using a Hybrid of Hydraulics and Machine Learning." *Scientific Reports* 10, no. 1: 8222. https://doi.org/10.1038/s41598-020-65232-5.

Huber, E. R., S. M. Carlson, and University of California, Berkeley. 2015. "Temporal Trends in Hatchery Releases of Fall-Run Chinook Salmon in California's Central Valley. San Francisco Estuary and Watershed." *Science* 13, no. 2: 1–23. https://doi.org/10.15447/sfews.2015v13iss2art3.

Irvine, J. R., M. R. Gross, C. C. Wood, L. B. Holtby, N. D. Schubert, and P. G. Amiro. 2005. "Canada's Species at Risk Act: An Opportunity to Protect Endangered Salmon." *Fisheries* 30, no. 12: 11–19. https://doi.org/10.1577/1548-8446(2005)30[11:CSARA]2.0.CO;2.

Ishida, K., A. Ercan, T. Trinh, et al. 2018. "Analysis of Future Climate Change Impacts on Snow Distribution Over Mountainous Watersheds in Northern California by Means of a Physically-Based Snow Distribution Model." *Science of the Total Environment* 645: 1065–1082. https://doi.org/10.1016/j.scitotenv.2018.07.250.

Jager, H. I., and K. A. Rose. 2003. "Designing Optimal Flow Patterns for Fall Chinook Salmon in a Central Valley, California, River." *North American Journal of Fisheries Management* 23: 1–21. https://doi.org/10.1577/1548-8675(2003)023<0001:DOFPFF>2.0.CO;2.

Jonsson, B., N. Jonsson, and L. P. Hansen. 2003. "Atlantic Salmon Straying From the River Imsa: STRAYING IN SALMON." *Journal of Fish Biology* 62, no. 3: 641–657. https://doi.org/10.1046/j.1095-8649.2003.00053.x.

Kammel, L. E., G. B. Pasternack, D. A. Massa, and P. M. Bratovich. 2016. "Near-Census Ecohydraulics Bioverification of (*Oncorhynchus mykiss*) Spawning Microhabitat Preferences." *Journal of Ecohydraulics* 1, no. 1–2: 62–78. https://doi.org/10.1080/24705357.2016.1237264.

Kassambara, A. (2022). Dunn's Test of Multiple Comparisons (0.7.0) [R].

Keefer, M. L., and C. C. Caudill. 2014. "Homing and Straying by Anadromous Salmonids: A Review of Mechanisms and Rates." *Reviews in Fish Biology and Fisheries* 24, no. 1: 333–368. https://doi.org/10.1007/s11160-013-9334-6.

Kim, B., B. F. Sanders, J. E. Schubert, and J. S. Famiglietti. 2014. "Mesh Type Tradeoffs in 2D Hydrodynamic Modeling of Flooding With a Godunov-Based Flow Solver." *Advances in Water Resources* 68: 42–61. https://doi.org/10.1016/j.advwatres.2014.02.013.

Kruskal, W. H., and W. A. Wallis. 1952. "Use of Ranks in One-Criterion Variance Analysis." *Journal of the American Statistical Association* 47, no. 260: 583–621. https://doi.org/10.1080/01621459.1952.10483441.

Lackey, R. T. 2017. *Science and Salmon Recovery. In new Strategies for Wicked Problems: Science and Solutions in the 21st Century*, 69–94. Corvallis, OR: Oregon State Universty Press. https://d1wqtxts1xzle7.cloudfront.net/54016039/2017a-Science-and-Salmon-Recovery-Reprint-Lackey-with-cover-page-v2.pdf?Expires=1648093750&Signature=FNWpMitygyc-MHIQ-X~sp-T6fQrXJL3fhcSPgcJh-pU~oxQv~W4DXw-0xDZi6fw8Rp4KqlMGMNUBx4dpTHvdMBUWsef3W7vjg9m1Jh1vo0QEV4ieZ5FXw2nP4pngJtR~HVnIRYQidqo5AdLlckT8kuHOx07USvQ53OusEp1xjCvQdgKsGC2vcK5yD2D~8NEc1S0RuirtcU3H16vmo6TK5IE8P-iSBGxgbeDtUKFqr8BbppuOeLPXcHQUm2v3kH~IYv-nQd4ABiR-Z6NVp8Zt7rCgTAHQRP803bQHZSWA3mRKplhc178wCXbHtq~tWOzOt8th7Q8QThBc-6SEH3qdkg__&Key-Pair-Id=APKAJLOHF5GGSLRBV4ZA.

Lamouroux, N., and Y. Souchon. 2002. "Simple Predictions of Instream Habitat Model Outputs for Fish Habitat Guilds in Large Streams: Habitat Modelling for Fish Guilds." *Freshwater Biology* 47, no. 8: 1531–1542. https://doi.org/10.1046/j.1365-2427.2002.00880.x.

Liaw, A., and M. Wiener. 2002. "Classification and Regression by randomForest." *R News* 2: 18–22.

Limerinos, J. T. 1970. *Determination of the Manning Coefficient From Measured bed Roughness in Natural Channels (GEOLOGICAL SURVEY WATER-SUPPLY PAPER 1898-B)*. Washington, DC: United States Geological Survey in cooperation with the California Department of Water Resources.

Liu, X. 2014. "Open-Channel Hydraulics: From Then to Now and Beyond." In *Modern Water Resources Engineering*, edited by L. K. Wang and C. T. Yang, 127–158. New York, NY: Humana Press. https://doi.org/10.1007/978-1-62703-595-8_2.

Lorenz, C. M., W. P. Cofino, and A. J. Gilbert. 2001. "Indicators for Transboundary River Management." *Environmental Management* 28, no. 1: 115–129. https://doi.org/10.1007/s002670010211.

Luis, S. M., and G. B. Pasternack. 2023. "Local Hydraulics Influence Habitat Selection and Swimming Behavior in Adult California Central Valley Chinook Salmon at a Large River Confluence." *Fisheries Research* 261: 106634. https://doi.org/10.1016/j.fishres.2023.106634.

Magilligan, F. J., and K. H. Nislow. 2005. "Changes in Hydrologic Regime by Dams." *Geomorphology* 71, no. 1–2: 61–78. https://doi.org/10.1016/j.geomorph.2004.08.017.

Magnhagen, C. 1988. "Predation Risk and Foraging in Juvenile Pink (*Oncorhynchus gorbuscha*) and Chum Salmon (O. Keta)." *Canadian Journal of Fisheries and Aquatic Sciences* 45, no. 4: 592–596. https://doi.org/10.1139/f88-072.

Marchetti, M. P., and P. B. Moyle. 2001. "Effects of Flow Regime on Fish Assemblages in a Regulated California Stream." *Ecological Applications* 11, no. 2: 530–539. https://doi.org/10.1890/1051-0761(2001)011[0530:EOFROF]2.0.CO;2.

Massey, F. J. 1951. "The Kolmogorov–Smirnov Test for Goodness of fit." *Journal of the American Statistical Association* 46, no. 253: 68–78. https://doi.org/10.1080/01621459.1951.10500769.

Matella, M. K., and A. M. Merenlender. 2015. "Scenarios for Restoring Floodplain Ecology Given Changes to River Flows Under Climate Change: Case From the San Joaquin River, California: Scenarios for Restoring Floodplain Ecology." *River Research and Applications* 31, no. 3: 280–290. https://doi.org/10.1002/rra.2750.

Middleton, C. T., S. G. Hinch, E. G. Martins, et al. 2018. "Effects of Natal Water Concentration and Temperature on the Behaviour of Up-River Migrating Sockeye Salmon." *Canadian Journal of Fisheries and Aquatic Sciences* 75, no. 12: 2375–2389. https://doi.org/10.1139/cjfas-2017-0490.

Miller, J. P. 1958. *High Mountain Streams: Effects of Geology on Channel Characteristics and bed Material (Interpretation of Quantitative Measurements Made in the Sangre de Cristo Range, North-Central new Mexico Memoir 4)*. Socorro, New Mexico: State Bureau of Mines and Mineral Resources and the New Mexico Institute of Mining and Technology.

Moir, H. J., C. N. Gibbins, C. Soulsby, and J. H. Webb. 2006. "Discharge and Hydraulic Interactions in Contrasting Channel Morphologies and Their Influence on Site Utilization by Spawning Atlantic Salmon (*Salmo salar*)." *Canadian Journal of Fisheries and Aquatic Sciences* 63, no. 11: 2567–2585. https://doi.org/10.1139/f06-137.

Moniz, P. J., G. B. Pasternack, D. A. Massa, L. W. Stearman, and P. M. Bratovich. 2019. "Do Rearing Salmonids Predictably Occupy Physical Microhabitat?," *Journal of Ecohydraulics* 1–19: 132–150. https://doi.org/10.1080/24705357.2019.1696717.

Moore, M. R., E. B. Maclin, and D. W. Kershner. 2001. "Testing Theories of Agency Behavior: Evidence From Hydropower Project Relicensing Decisions of the Federal Energy Regulatory Commission." *Land Economics* 77, no. 3: 423–442. https://doi.org/10.2307/3147134.

Mount, J. F. 1995. *California Rivers and Streams: The Conflict Between Fluvial Process and Land use*. Berkeley, CA: University of California Press.

Moursund, R. A., T. J. Carlson, and R. D. Peters. 2003. "A Fisheries Application of a Dual-Frequency Identification Sonar Acoustic Camera." *ICES Journal of Marine Science* 60, no. 3: 678–683. https://doi.org/10.1016/S1054-3139(03)00036-5.

Moyle, P. B., M. P. Marchetti, J. Baldrige, and T. L. Taylor. 1998. "Fish Health and Diversity: Justifying Flows for a California Stream." *Fisheries* 23, no. 7: 6–15. https://doi.org/10.1577/1548-8446(1998)023<0006:FHADJF>2.0.CO;2.

Murdoch, A. R., M. A. Tonseth, and T. L. Miller. 2009. "Migration Patterns and Spawning Distribution of Adult Hatchery Sockeye Salmon Released as Parr From Net-Pens in Lake Wenatchee, Washington." *North American Journal of Fisheries Management* 29, no. 2: 447–459. https://doi.org/10.1577/M08-051.1.

Nalin, R., and M. Kotulla. 2018. *Rapid Bedrock Incision by Water Stream Outburst: The Case of the Oroville Dam (California, USA)*. Loma Linda, CA: Geoscience Research Institute. https://www.grisda.org/rapid-bedrock-incision-by-water-stream-outburst-the-case-of-the-oroville-dam-california-usa-1.

Naman, S. M., J. S. Rosenfeld, J. R. Neuswanger, E. C. Enders, and B. C. Eaton. 2019. "Comparing Correlative and Bioenergetics-Based Habitat Suitability Models for Drift-Feeding Fishes." *Freshwater Biology* 64, no. 9: 1613–1626. https://doi.org/10.1111/fwb.13358.

Narum, S. R., T. L. Schultz, D. M. Van Doornik, and D. Teel. 2008. "Localized Genetic Structure Persists in Wild Populations of Chinook Salmon in the John Day River Despite Gene Flow From Outside Sources." *Transactions of the American Fisheries Society* 137, no. 6: 1650–1656. https://doi.org/10.1577/T07-232.1.

National Marine Fisheries Service. 2014. *Recovery Plan for the Evolutionarily Significant Units of Sacramento River Winter-Run Chinook Salmon and Central Valley Spring-Run Chinook Salmon and the Distinct Population Segment of California Central Valley Steelhead*. Sacramento, CA: National Marine Fisheries Service.

National Marine Fisheries Service. 2016. *Endangered Species Act Section 7(a)(2) Biological Opinion, and Magnuson-Stevens Fishery Conservation and Management Act Essential Fish Habitat Response and Fish and Wildlife Coordination Act Recommendations for Relicensing the Oroville Facilities Hydroelectric Project, Butte County California FERC Project No. 2100-134*. Sacramento, CA: U.S. Department of Commerce. WCR-2015-3218.

Nestler, J. M., R. T. Milhous, T. R. Payne, and D. L. Smith. 2019. "History and Review of the Habitat Suitability Criteria Curve in Applied Aquatic Ecology: Review of Habitat Suitability Criteria in Aquatic Ecology." *River Research and Applications* 35, no. 8: 1155–1180. https://doi.org/10.1002/rra.3509.

Ostertagová, E., O. Ostertag, and J. Kováč. 2014. "Methodology and Application of the Kruskal-Wallis Test." *Applied Mechanics and Materials* 611: 115–120. https://doi.org/10.4028/www.scientific.net/AMM.611.115.

Pasternack, G. B. 2019a. "Applied Fluvial Ecohydraulics." In *Environmental Science*, edited by G. B. Pasternack. Oxford: Oxford University Press. https://doi.org/10.1093/obo/9780199363445-0124.

Pasternack, G. B. 2019b. "Natural Fluvial Ecohydraulics." In *Environmental Science*, edited by G. B. Pasternack. Oxford: Oxford University Press. https://doi.org/10.1093/obo/9780199363445-0111.

Penna, N., M. De Marchis, O. Canelas, E. Napoli, A. Cardoso, and R. Gaudio. 2018. "Effect of the Junction Angle on Turbulent Flow at a Hydraulic Confluence." *Water* 10, no. 4: 469. https://doi.org/10.3390/w10040469.

Persinger, J. W., D. J. Orth, and A. W. Averett. 2011. "Using Habitat Guilds to Develop Habitat Suitability Criteria for a Warmwater Stream Fish Assemblage." *River Research and Applications* 27, no. 8: 956–966. https://doi.org/10.1002/rra.1400.

Powell, J. H., and M. R. Campbell. 2020. "Contemporary Genetic Structure Affects Genetic Stock Identification of Steelhead Trout in the Snake River Basin." *Ecology and Evolution* 10, no. 19: 10520–10531. https://doi.org/10.1002/ece3.6708.

R Core Team. 2023. *R: A Language and Environment for Statistical Computing*. [Computer software. Vienna, Austria: R Foundation for Statistical Computing. https://cran.r-project.org/.

Richards, K. S. 1980. "A Note on Changes in Channel Geometry at Tributary Junctions." *Water Resources Research* 16, no. 1: 241–244. https://doi.org/10.1029/WR016i001p00241.

Salinger, D. H., and J. J. Anderson. 2006. "Effects of Water Temperature and Flow on Adult Salmon Migration Swim Speed and Delay." *Transactions of the American Fisheries Society* 135, no. 1: 188–199. https://doi.org/10.1577/T04-181.1.

Santos, N. R., J. V. E. Katz, P. B. Moyle, and J. H. Viers. 2014. "A Programmable Information System for Management and Analysis of Aquatic Species Range Data in California." *Environmental Modelling & Software* 53: 13–26. https://doi.org/10.1016/j.envsoft.2013.10.024.

Schaller, H. A., C. E. Petrosky, and E. S. Tinus. 2014. "Evaluating River Management During Seaward Migration to Recover Columbia River Stream-Type Chinook Salmon Considering the Variation in Marine Conditions." *Canadian Journal of Fisheries and Aquatic Sciences* 71, no. 2: 259–271. https://doi.org/10.1139/cjfas-2013-0226.

Schwindt, S., G. B. Pasternack, P. M. Bratovich, G. Rabone, and D. Simodynes. 2019. "Hydro-Morphological Parameters Generate Lifespan Maps for Stream Restoration Management." *Journal of Environmental Management* 232: 475–489. https://doi.org/10.1016/j.jenvman.2018.11.010.

Segal, M. R. 2004. *Machine Learning Benchmarks and Random Forest Regression [UCSF: Center for Bioinformatics and Molecular Biostatistics]*. San Francisco: University of California. https://escholarship.org/uc/item/35x3v9t4.

Silva, P. V., and G. B. Pasternack. 2018. *Lower Yuba River Topographic Mapping Report*. Prepared for the Yuba Water Agency. Davis, CA: University of California Davis.

Simon, A., and M. Rinaldi. 2006. "Disturbance, Stream Incision, and Channel Evolution: The Roles of Excess Transport Capacity and Boundary Materials in Controlling Channel Response." *Geomorphology* 79, no. 3–4: 361–383. https://doi.org/10.1016/j.geomorph.2006.06.037.

Stadler, J. H., and D. P. Woodbury. 2009. "Assessing the Effects to Fishes From Pile Driving: Application of new Hydroacoustic Criteria." In *INTER-NOISE and NOISE-CON Congress and Conference Proceedings*, vol. 2, 4724–4731. Ottawa, Canada: Institute of Noise Control Engineering.

Strange, J. S. 2010. "Upper Thermal Limits to Migration in Adult Chinook Salmon: Evidence From the Klamath River Basin." *Transactions of the American Fisheries Society* 139, no. 4: 1091–1108. https://doi.org/10.1577/T09-171.1.

Sturrock, A. M., W. H. Satterthwaite, K. M. Cervantes-Yoshida, et al. 2019. "Eight Decades of Hatchery Salmon Releases in the California Central Valley: Factors Influencing Straying and Resilience." *Fisheries* 44, no. 9: 433–444. https://doi.org/10.1002/fsh.10267.

Sun, F., N. Berg, A. Hall, M. Schwartz, and D. Walton. 2019. "Understanding end-Of-Century Snowpack Changes Over California's Sierra Nevada." *Geophysical Research Letters* 46, no. 2: 933–943. https://doi.org/10.1029/2018GL080362.

Suzuki, H. 2006. "Legal Systems to Protect Salmon in the United States and Japan." *Hokkai Gakuen University Law Research* 41, no. 4: 898–934.

Tharme, R. E. 2003. "A Global Perspective on Environmental Flow Assessment: Emerging Trends in the Development and Application of Environmental Flow Methodologies for Rivers." *River Research and Applications* 19, no. 5–6: 397–441. https://doi.org/10.1002/rra.736.

Tierney, K. B., D. H. Baldwin, T. J. Hara, P. S. Ross, N. L. Scholz, and C. J. Kennedy. 2010. "Olfactory Toxicity in Fishes." *Aquatic Toxicology* 96, no. 1: 2–26. https://doi.org/10.1016/j.aquatox.2009.09.019.

Tierney, K. B., J. L. Sampson, P. S. Ross, M. A. Sekela, and C. J. Kennedy. 2008. "Salmon Olfaction Is Impaired by an Environmentally Realistic Pesticide Mixture." *Environmental Science & Technology* 42, no. 13: 4996–5001. https://doi.org/10.1021/es800240u.

Trenberth, K. 2011. "Changes in Precipitation With Climate Change." *Climate Research* 47, no. 1: 123–138. https://doi.org/10.3354/cr00953.

Ueda, H. 2011. "Physiological Mechanism of Homing Migration in Pacific Salmon From Behavioral to Molecular Biological Approaches." *General and Comparative Endocrinology* 170, no. 2: 222–232. https://doi.org/10.1016/j.ygcen.2010.02.003.

Unwin, M. J., and T. P. Quinn. 1993. "Homing and Straying Patterns of Chinook Salmon (Oncorhynchus Tshawytscha) From a new Zealand Hatchery: Spatial Distribution of Strays and Effects of Release Date." *Canadian Journal of Fisheries and Aquatic Sciences* 50, no. 6: 1168–1175. https://doi.org/10.1139/f93-133.

Vähä, J.-P., J. Erkinaro, E. Niemelä, and C. R. Primmer. 2007. "Life-History and Habitat Features Influence the Within-River Genetic Structure of Atlantic Salmon." *Molecular Ecology* 16, no. 13: 2638–2654. https://doi.org/10.1111/j.1365-294X.2007.03329.x.

van Poorten, B. T., S. P. Cox, and A. B. Cooper. 2013. "Efficacy of Harvest and Minimum Size Limit Regulations for Controlling Short-Term Harvest in Recreational Fisheries." *Fisheries Management and Ecology* 20, no. 2–3: 258–267. https://doi.org/10.1111/j.1365-2400.2012.00872.x.

Wampler, P. 1986. *Development of Habitat Preference Criteria for Holding Adult Spring Chinook Salmon [Fisheries Assistance Office*. Olympia, WA: U.S. Fish and Wildlife Service.

Williams, G. 2011. "Random Forests." In *Data Mining With Rattle and R*, edited by I. G. Williams, 245–268. New York: Springer. https://doi.org/10.1007/978-1-4419-9890-3_12.

Xu, C., N. G. McDowell, R. A. Fisher, et al. 2019. "Increasing Impacts of Extreme Droughts on Vegetation Productivity Under Climate Change." *Nature Climate Change* 9, no. 12: 948–953. https://doi.org/10.1038/s41558-019-0630-6.

Yuan, S., L. Xu, H. Tang, Y. Xiao, and C. Gualtieri. 2022. "The Dynamics of River Confluences and Their Effects on the Ecology of Aquatic Environment: A Review." *Journal of Hydrodynamics* 34, no. 1: 1–14. https://doi.org/10.1007/s42241-022-0001-z.

Yuba Accord River Management Team. 2013. *Aquatic Resources of the Lower Yuba River: Past, Present, and Future [Draft Interim Report]*. Sacramento, CA: Yuba Accord Monitoring and Evaluation Program. http://www.yubaaccordrmt.com/Interim%20ME%20Report/ME%20Interim%20Report_Draft_April%202013.pdf.

Zeug, S. C., K. Sellheim, C. Watry, J. D. Wikert, and J. Merz. 2014. "Response of Juvenile Chinook Salmon to Managed Flow: Lessons Learned From a Population at the Southern Extent of Their Range in North America." *Fisheries Management and Ecology* 21, no. 2: 155–168. https://doi.org/10.1111/fme.12063.

Zhang, H., G. Jin, and Y. Yu. 2018. "Review of River Basin Water Resource Management in China." *Water* 10, no. 4: 425. https://doi.org/10.3390/w10040425.

Supporting Information

Additional supporting information can be found online in the Supporting Information section.